2012

Studying Antimicrobial Peptide Mechanisms: Analysis of Novel HDAPS and Development of High-Throughput Techniques

Kathryn Pavia
Wellesley College, kpavia@wellesley.edu

Studying Antimicrobial Peptide Mechanisms: Analysis of Novel HDAPS and Development of High-Throughput Techniques

Kathryn E. Pavia
Advisor: Donald E. Elmore

Submitted in Partial Fulfillment
of the Prerequisite for Honors
In Biological Chemistry

Wellesley College
April, 2012

This page has been in the making (at least mentally) for about 3 years now because it would be impossible to have finished this thesis without an enormous support network. Fortunately this is one area where I have been extraordinarily blessed.

First and foremost an enormous thanks to Professor Elmore for starting me on this journey three and a half long years ago and for being the most wonderful advisor imaginable on this voyage. Whether troubleshooting experiments, critiquing presentations, coping with day-to-day crises, letting me de-stress by playing with your baby, or even just chatting in the hallways, I couldn't possibly have asked for a funnier, more supportive advisor. I can never thank you enough for everything you have done and for making research one of the best parts of my time at Wellesley!

Thank you to my wonderful committee members, Nancy Kolodny and Gary Harris for your helpful input, edits, and encouragement.

Thank you to HoiSee, Allison, and Ryann for being mentors, teachers, role models, and big sisters when I was new and nervous. You may not know it, but your support, advice, and friendship meant an enormous amount during my first semesters. Thanks to Yoonie, Amanda, Liz, Julia, Ali, Penny, and Amy for making lab a place of laughter, music, decorations, and friendship. Special thanks to Maria Bustillo for indulging my crafty side, cheering me up with poetry, and making distribution requirements bearable. Enormous thanks to Sara Spinella for being a listening ear, an amazing collaborator, and the other half of my brain; for book recommendations, life advice, philosophical discussions, and always showing me what's coming next. I'm so grateful that you've been here with me for the whole run.

For daily support and love, I owe enormous thanks Kyla, Emma, and Devika for being there every step of the way for all four years and for reminding me about life outside the lab. Special thanks to Kyla for being the most amazing suite-mate ever and for always knowing how to de-escalate a panicked scientist. Thank you for adopting me on holidays, bribing me with delicious treats, making goal charts, having spontaneous dance parties and TV breaks at all hours, and everything else you do on a daily basis. I could never have done this without you- any sanity I have left today is 100% yours.

Finally I wouldn't be where I am today without the love and confidence of my family. Thank you guys for unfailing faith, support, and willingness to listen to incomprehensible biochemistry. I owe a particular debt to my mom for making me into the woman I am today, for all of her love and sacrifices, and for making the prospect of "turning into your mother" something to embrace.

TABLE OF CONTENTS

TABLES AND FIGURES

ABBREVIATIONS

AMP: Antimicrobial Peptide
BF2: Buforin II
CPP: Cell-Penetrating Peptide
DesHDAP: Designed Histone-Derived Antimicrobial Peptide
DPA: Dipicolinic Acid
DNS-PE: 5-dimethylaminonaphthalene-1-sulfonyl phosphatidylethanolamine
FRET: Fluorescence Resonance Energy Transfer
HTS: High-Throughput Screening
LB: Luria Broth
PC: Phosphatidylcholine
PG: phosphatidylglycerol
PI: Propidium Iodide
RDA: Radial Diffusion Assay
TO: Thiazole Orange
TSB: Tryptic Soy Broth

Abstract

Previously novel histone-derived antimicrobial peptides (HDAPs) were designed based on properties of Buforin 2, a peptide whose activity depends on membrane translocation, and DesHDAP1 and DesHDAP3 showed significant antibacterial activity. Their DNA binding, permeabilization, and translocation abilities were assessed independently and compared to antibacterial activity to determine whether the HDAPs share a mechanism with BF2. DesHDAP1 translocates effectively across lipid vesicle membranes while DesHDAP3 translocates poorly, and none of the DesHDAPs show significant membrane perturbation. Further investigation into the role of the proline hinge suggested that a proline hinge can promote membrane translocation in some peptides, but that the extent of its effect on permeabilization depends on the peptide's amphipathic properties. In order to extend the scope of antimicrobial peptide screening in the Elmore lab, antimicrobial activity, permeabilization, and translocation screens compatible with high-throughput plate-reader software were also developed. While the initial antimicrobial activity and permeabilization screens attempted were not appropriate for this system, translocation screening was easily adapted to the plate-reader platform. Ultimately information about novel HDAPs provides insight into the potential mechanisms of such peptides, while development of high-throughput techniques extends the capacity to explore and analyze novel peptide libraries.

1. INTRODUCTION

1.1 Modern Antimicrobial Agents and Resistance

The majority of antibiotics in use today were discovered between the 1930's and the 1960's or are closely related chemical derivatives of these initial antibiotics[1]. However in the more than half century since their discovery many of these antibiotics have been rendered obsolete by the emergence of antibiotic-resistant bacteria. *M. tuberculosis* and *S. aureus* are both common infectious agents that have developed clinically relevant strains resistant to currently prescribed antibiotics. Multi-drug resistant tuberculosis accounts for an increasing percentage of tuberculosis diagnoses worldwide, with levels approaching 18% in certain eastern European countries[2]. Methicillin resistant *S. aureus* (MRSA) infections are frequent, accounting for 58% of *S. aureus* hospitalizations, and very serious, causing nearly 19,000 deaths in 2004[3]. Although MRSA was once known as a common hospital acquired infection, it has increasingly been observed in non-hospitalized populations[4].

Bacteria develop antibacterial resistance either through mutation of existing genes or acquisition of resistance genes from other bacteria in the population. Antibiotic resistance may be the result of a change to the antibiotic binding site, acquisition of the ability to break down or export an antibiotic, or development of pathways that allow a bacteria to tolerate the inactivation of the antibiotic target[5]. For example β-lactamase enzymes hydrolyze the β-lactam ring in antibiotics such as ampicillin and cephalosporin[6], a single mutation to RNA polymerase renders rifampin inactive[7], and mutations to the 23S ribosomal subunit greatly decrease the binding affinity of macrolide antibiotics like erythromycin[8].

The emergence of antibiotic resistant bacterial strains has not been met with an equivalent burst in the discovery of new antibacterial therapeutics. This discrepancy has been

attributed to exhaustion of traditional antibiotic sources such as soil bacteria or fungal secretions as well as to financial considerations that lead pharmaceutical companies to allocate development resources toward medicines that will be taken on an ongoing basis and will therefore return greater profit[9]. The resulting imbalance between antibiotic resistant organisms and effective antibiotics has encouraged a push within the scientific community to promote the identification and development of novel antibacterial agents[10].

1.2 Antimicrobial Peptides

Antimicrobial peptides (AMPs) have recently risen to the attention of many researchers as a promising new avenue for therapeutic development. These peptides are used in the innate immune systems of many organisms, including fish[11,12], amphibians[13,14], insects[15], and mammals[16]. The defining feature of these peptides is a length of between 12-100 amino acids and a net positive charge of between +2 and +9. As of January 2012, the antimicrobial peptide database has recorded over 1900 antimicrobial peptides from natural sources[17].

While peptides can have antimicrobial activity against viruses, fungi, and even cancerous cells, much of the research to date has focused particularly on peptides with antibacterial activity, as will this thesis. In order to be effective therapeutic agents, AMPs must be biologically stable and capable of preferentially killing bacterial cells without simultaneously exerting harmful effects on healthy mammalian cells. Both of these properties are of concern for AMP development and are frequent goals of targeted modifications. While susceptibility to biological proteases is difficult to eliminate, the sequence of AMPs does play an important, though poorly understood, role in prokaryotic cell targeting. Greater understanding of AMP mechanisms is critical to eventual efforts toward designing more effective peptides.

The cationic nature of antimicrobial peptides seems to be particularly important for AMP activity. The net positive charge of AMPs assists in bacterial membrane targeting via electrostatic interactions because bacterial membranes have a higher content of negatively charged lipid head groups such as phosphatidylglycerol (PG) and a greater negative transmembrane potential than do healthy mammalian cells[18]. An additional factor contributing to the observed preference of AMPs for prokaryotic cells is the fact that cholesterol, which is found in eukaryotic but not prokaryotic cell membranes, seems to inhibit the activity of antimicrobial peptides[19].

While cationic character is important to the function of AMPs, there does appear to be an optimal charge. Using the helical peptide L-V13K, Jiang et al investigated the role of net charge on the peptide's antibacterial and hemolytic properties[20]. The paper investigated the effects of changing the net charge of V13K, which normally has a net charge of +7, to net charges ranging from -5 to +10. Unsurprisingly, lowering the net charge to +4 or below completely eliminated the antibacterial activity of the peptide. As the net charge increased from +7 to +10 the antibacterial activity increased; however while the +8 peptide had minimal hemolytic activity, both the +9 and +10 peptides were extremely hemolytic. This suggests that there may be an optimum charge for the creation of useful therapeutics capable of targeting bacterial membranes without exerting harmful effects on host cells.

Antimicrobial peptides can adopt many conformations including alpha helices, beta sheets, polyproline extended helices, random coils, and loops stabilized by disulfide bridges. Alpha helical peptides are both common and extremely well studied, particularly in relationship to the optimal distribution of residues about helical faces. While Park et al observed a direct correlation between alpha helicity and antimicrobial activity from their study of truncations of

Buforin 2[21], this does not appear to be a universal trend. For example increasing the hydrophobic content of the helical peptide V13K led the peptides to adopt more helical conformations, but also produced higher self-aggregation and hemolytic behaviors[22]. Other histone-derived antimicrobial peptides have also failed to exhibit this correlation between peptide helicity and general antimicrobial activity[23].

Although the net charge and conformation of AMPs play important roles in their activity, the most important parameter may be the distribution of the charges and hydrophobic residues about the helix. Studies suggest that an amphipathic charge distribution with defined cationic and hydrophobic faces is optimal for AMP activity[22]. Peptides with segregated areas of charged residues and hydrophobic residues can target and interact with the cell membrane electrostatically through their cationic side chains and insert into or cross the lipid bilayer because of favorable interactions between hydrophobic regions of the peptide and lipid tails. However, excessive hydrophobic character can lead to peptide aggregation and hemolysis.

Antimicrobial peptides have several potential advantages as therapeutic agents. Many AMPs are active against a broad range of medically relevant bacteria, and some also demonstrate selective ability to target and kill fungal or cancerous cells[24]. Antimicrobial peptides target nonspecific cell components such as the cell membrane, making it difficult for bacteria to develop resistance through minor mutations.

The fact that AMPs have existed as a part of innate immune systems for so many years demonstrates that they are robust antimicrobial agents. However, this has also given ample time for certain microorganisms to develop mechanisms to resist AMP lethal effects. Some bacteria manage to reduce their overall membrane surface charge, preventing the initial electrostatic attraction, while others encode enzymes for proteolytic degradation of AMPs[25]. However, the

continued efficacy of AMPs against wide ranges of infectious organisms suggests that AMP resistance may be less common and easily evolved than resistance to traditional antibiotics.

1.3 AMP Mechanisms

Antimicrobial peptides are characterized by 3 general mechanisms of bactericidal action resulting from interaction between the peptide and the bacterial membrane. The first two mechanisms both involve loss of membrane barrier function as the primary cause of cell death (figure 1). First, peptides may cause nonspecific membrane disruption in a detergent-like fashion, as in the "carpet model"[26]. Secondly peptides may associate with each other to form well-defined pores across the membrane through which fluids and important solutes can pass, described by "toriodal pore"[27] and "barrel-stave"[28] models. While both of these models propose a stable pore of aggregated peptide, they differ in the conformation of the membrane lipids around the pore and the membrane-lipid interactions. In the barrel-stave model there is no membrane deformation, so the peptide pore contacts the phospholipid heads near either edge of the membrane and the hydrophobic tails in the middle of the membrane (figure 1B). In contrast, the torroidal pore model suggests that lipids deform inwards around the pore such that only the head groups are in contact with the peptide at any point on the pore (figure 1C).

Magainin II is a 23 amino acid helical AMP initially isolated from *Xenopus laevis*[14], which has been particularly well characterized through ongoing efforts to understand the mechanisms of lytic peptides. NMR and fluorescence quenching experiments have shown that magainin initially associates with bacteria in an orientation parallel to the plane of the membrane before aggregating and inserting into the membrane once a critical peptide/lipid ratio is

reached[19]. The resulting membrane pores allow K^+ efflux and loss of barrier function, ultimately leading to cell death.

Many biological signaling molecules interact with and cross cell membranes through binding to specific receptors. In order to assess whether AMP interactions with bacterial membranes depend on recognition of specific receptors or lipid binding sites, researchers turned to the chiral properties of amino acids and protein secondary structures. Amino acids, lipid head groups, and protein secondary structures are chiral and as a result interact specifically with other chiral molecules. This is an important issue in drug design, as often only one enantiomer is capable of effectively binding to the required biological target. If AMP interactions with bacterial cells were mediated through specific receptors or particular interactions with lipid heads, D- and L- enantiomers would show different antibacterial activities. However when AMPs composed entirely from D-amino acids were compared to their L-amino acid counterparts, the same antibacterial activity and selectivity were observed[29]. Thus AMPs target and interact with cellular membranes through a mechanism that does not depend on specific recognition of chiral proteins or lipids. This assertion is further supported by the ability of peptides to interact with lipid vesicles, which have only the phospholipids without any of the receptors or proteins found in living cell membranes.

The third mechanism by which AMPs may exert their antimicrobial activity differs from the previous two in that it does not rely on a loss of barrier function to kill the bacterial cell. Instead, these AMPs cross the cell membrane without grossly disrupting the membrane integrity. Once the peptides reach the cell interior, they can execute their bactericidal function through interfering with any number of essential cellular processes. Although they are less common, AMPs that exert their activity by crossing the cell membrane and interacting with intracellular

components have many therapeutically promising features. The intracellular activity means that these peptides address a wide range of targets. AMPs that use this mechanism include indolicidin, a neutrophil-derived AMP that inhibits bacterial DNA synthesis[30] and proline-rich peptides whose intracellular target(s) have not been identified[31].

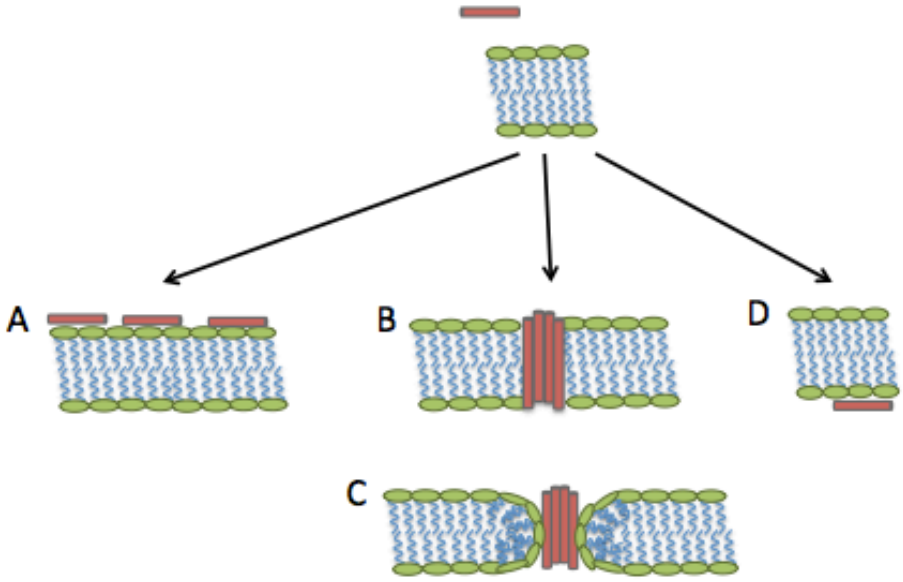

Figure 1: Commonly accepted antibacterial mechanisms of AMPs. Upon approaching the membrane, the peptides may align parallel to the membrane (A), insert into the membrane perpendicular to the membrane plane (B-C), or cross the membrane and enter the cell (D). Note that in the barrel-stave mechanism (B) the lipid heads and hydrophobic tails come in contact with the peptide pore, whereas in the toroidal pore mechanism (C) the lipid membrane curves inward such that only the lipid heads contact the peptide.

1.4 Histone Derived Antimicrobial Peptides

BF2, the most thoroughly studied membrane-translocating AMP, is derived from a defensive peptide identified in the stomach of the giant toad *Bufo bufo garagrizans* and shows broad spectrum activity against gram positive and gram negative bacteria[13]. BF2 is capable of entering bacterial cells without significantly disrupting their membranes[21] through a process dependent on the presence of a helix-breaking proline residue[32]. The proline residue disrupts the

helical structure of BF2, allowing it more flexibility to adopt ideal amphipathic conformation in contact with cell membranes. Proline seems to be ideally situated in its position as the 11th residue in the peptide, as moving it one turn towards either the N- or C- terminus of the peptide results in a dramatic decrease in antibacterial strength[33].

Interestingly, BF2 shares complete sequence homology to a DNA binding portion of histone H2A and has a high affinity for DNA. BF2's antimicrobial activity is dependent on its DNA-binding ability, as evidenced by a dramatic decrease in antimicrobial activity when important DNA binding residues are altered[34]. Although BF2 itself does not show appreciable anti-cancer activity, a synthetic analog consisting of buforin II with a deletion of the N-terminal random coil and an extension of the C-terminal [RLLR] repeat showed both antibacterial activity comparable to that of BF2[32] as well as potent activity against more than 60 types of cancerous cells[35].

The potency of BF2 suggested that histones might be a promising and largely unexplored source of template material for the design of antimicrobial peptides. Whole histones display some antimicrobial properties, are capable of entering cells without causing membrane disruption, and have even been used as transfection agents to deliver DNA cargoes to intracellular targets[36]. Both whole histones and peptides homologous to histone fragments have been identified as components of innate immunities[37]. Several antimicrobial peptides with sequence homology to histone subunits have been isolated from natural sources, including parasin from catfish[11], hipposin from Atlantic halibut[12], and onchorhyncin II from rainbow trout[38].

Based on the properties of BF2 that are required for antibacterial activity, Tsao et al designed three novel histone-derived antimicrobial peptides homologous to DNA-binding

portions of histone subunits[23]. Each peptide was chosen for its predominantly helical structure broken by a proline hinge as well as the presence of multiple positive charges. When tested, the three novel peptides all displayed activity against a range of gram-positive and -negative bacteria. Interestingly, the peptides demonstrate different patterns of efficacy against particular bacterial strains. Furthermore differential changes to turbidity upon peptide addition suggest that the three peptides may not share an antimicrobial mechanism EXPAND. While this small-scale design success suggests the utility of histones as design templates for rational creation of novel AMPs, there has not yet been any systematic analysis of histones as source material for antimicrobial peptides.

1.5 Cell Penetrating Peptides

A closely related and sometimes overlapping class of peptides with therapeutic potential are cell penetrating peptides (CPPs) (figure 2). Like AMPs, these small peptides interact with cell membranes through electrostatic interactions, but many CPPs cross the lipid bilayer and enter into the cell interior without causing any membrane disruption or adversely affecting the cell. CPPs are of interest as delivery vectors because they can be covalently or electrostatically bound to cargo, which they then transport with them to the interior of the cell. This process has been successfully used to

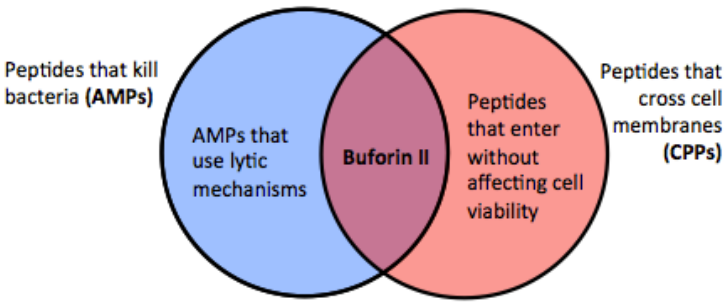

Figure 2: Although they are sometimes addressed as completely separate areas of research, AMPs and CPPs overlap in the form of cell-penetrating AMPs such as BF2.

promote the uptake of molecules such as small molecule pharmaceuticals[39], siRNA[40,41], proteins[41], or liposomes[42].

Like AMPs, CPPs are short and usually contain cationic and hydrophobic residues arranged in an amphipathic conformation[43]. Although the role of endocytosis in CPP uptake is a topic of ongoing investigation, it appears that the electrostatic interaction between charged residues and cell membranes is important to CPP targeting and activity[44]. In the case of eukaryotic cells, it is hypothesized that negatively charged heparin sulfate is the important attractor, supported by the observation that cells lacking heparin sulfate show reduced internalization of CPPs[45].

In contrast to this general trend, one anionic CPP has been described. SAP (E) was created by replacing each arginine in the SAP peptide with glutamine, forming a peptide with an extended polyproline helix and a net charge of -3 [46]. This peptide was efficiently internalized into 4 cancerous cell lines through a mechanism that showed minimal dependence on the presence of heparin sulfate, suggesting that at least some CPPs may not use electrostatic attractions to mediate initial cellular approach. As with AMPs, investigators still have no method for design or prediction of CPPs based on conserved features or sequences.

1.6 Peptide Discovery and Modification

Naturally occurring antimicrobial peptides, identified though analysis of mucous membrane secretions or organ tissue samples from various organisms, account for the majority of AMPs in the literature. However, after the initial discovery, many studies look at particular fragments of or substitutions to these peptides in order to learn about the peptides' mechanisms. Alterations that reduce or eliminate antimicrobial activity provide information about portions of

the peptide that are important to antibacterial activity and are often used in the determination of the peptide's mechanism of action.

Many research groups have sought specific mutations that could improve desired characteristics of AMPs. Ideal therapeutic treatments must not only have broad spectrum activity against pathogens, but must also be soluble, resistant to degradation *in vivo*, and minimally harmful to healthy cells. Of particular concern to the AMP community are the issues of enzymatic degradation of AMPs by proteases and detrimental effects of AMPs on mammalian cells (usually measured by hemolysis of red blood cells).

One particularly promising trend that appears to jointly address the issues of hemolytic activity and susceptibility to enzymatic degradation is the incorporation of D-amino acids into AMPs. Naturally produced proteins are composed exclusively of L- amino acids, but the D-enantiomers can be chemically synthesized. AMPs synthesized with one or more D-amino acids have demonstrated equivalent antimicrobial activity compared to their L-enantiomers while resisting proteolytic degradation[47–49]. Single D-amino acid substitutions can also affect the folding of a peptide[50], while peptides composed entirely of D-amino acids retain the same secondary structure with opposite chirality as compared to their L-enantiomers[47]. In particular the increased resistance to proteolytic degradation suggests that incorporation of D-amino acids might be a promising avenue for AMP therapeutic development.

Other unnatural amino acid substitutions have also been investigated in hopes of improving *in vivo* peptide stability. Fluorinated analogs of buforin and magainin retained antimicrobial activity comparable to the unmodified peptides and exhibited greater resistance to degradation by trypsin[51]. In the case of the buforin analogs, fluorinated peptides also displayed greatly reduced hemolytic activity. While such studies are able to make important and relevant

improvements to the activities of current AMPs, they are limited by issues such unnatural amino acid availability and peptide synthesis, which limit the number of modified peptides that can reasonably be tested in a single experimental design.

1.7 High Throughput Screening for Antimicrobial Discovery

Antimicrobial peptides used for research are usually chemically synthesized, and one of the limiting factors in AMP research is the high cost of peptide production. However, despite the short length of AMPs, the number of naturally occurring amino acids means that the field of potential peptides is extremely large. Many studies have focused on truncating, fusing, or making specific substitutions to peptides discovered from natural sources. However, despite the number of AMPs described to date, our ability to predict or design novel AMPs remains poor.

Although scientists lack a global understanding of the features that make an effective antimicrobial peptide, some peptides designed from repeating elements that occur frequently in AMPs have demonstrated antimicrobial activity. Xie et al identified two commonly recurring motifs among membrane-binding peptides from a random peptide library and demonstrated that peptides composed of 6 repetitions of the motifs showed both antimicrobial activity and prokaryotic membrane selectivity[52]. While investigating the properties of BF2, Park et al identified the C-terminal helical region as a motif characteristic of its antimicrobial activity and noted that a peptide composed of 5 repetitions of this 4 amino-acid motif showed strong antibacterial activity against a range of bacterial strains[21].

In order to efficiently identify novel AMPs and add to the data regarding the properties that create an effective antimicrobial peptide, many research groups have turned to high throughput screening (HTS). HTS techniques use 96 or 384 well plates to screen small volumes

of potentially active compounds using assays that can detect desirable traits with plate reader software. Kim and Cha used a fusion of enhanced cyan and yellow fluorescence proteins to identify proteins with membrane permeabilization activity by monitoring a decrease in fluorescence resonance energy transfer (FRET) fluorescence[53]. Under neutral pH conditions, such as those within an intact cell this protein was capable of transferring energy from the cyan protein to the yellow protein because both were stable and correctly folded. However, in lower pH conditions the yellow fluorescent protein became unstable and was no longer able to accept energy transfer from the cyan protein. Thus when bacterial cells were suspended in a solution with a lower external pH, membrane permeabilization was identifiable by the decrease in FRET as the fusion protein from lysed cells unfolded in the low pH environment. This technique was capable not only of identifying peptides with membrane-lytic properties but also of characterizing dose-response curves and quantitative analysis.

Advances in analytical instruments and computational power have enabled exciting new screening techniques for the analysis of enormous datasets of visual material. One emerging technique, called high-content screening, images fluorescently labeled cells from each well of 96 or 384 well plates then uses complex image analysis software to detect morphological changes based on defined parameters such as changes in shape or internalization and localization of labeled molecules[54]. While this analysis technique requires specialized microscopy equipment, image analysis programs, and data storage, it has the promising ability to collect data in representative infectious scenarios such as the invasion of eukaryotic cells by bacteria. Additionally, separate stains for eukaryotic nuclei and invasive bacteria allow the simultaneous evaluation of cytotoxicity and antibacterial activity in an *in vivo* system.

Other studies have approached AMP discovery using the simplified system of isolated lipid vesicles to identify peptides that lyse or cross lipid bilayers. Wimley et al used vesicle leakage to identify 10 soluble membrane active peptides from a library of 16,384 peptides[55]. These peptides also showed broad-spectrum antimicrobial activity despite significant variation in length, net charge, and helical content[56]. In a subsequent study, the group used an orthogonal screen to simultaneously monitor membrane permeabilization through the chelation of terbium (III) and dipicolinic acid (DPA) and peptide translocation through chymotrypsin cleavage of an AMC fluorophor[57]. This assay identified 18 peptides capable of crossing lipid bilayers without causing significant membrane leakage. These peptides did not bear any resemblance to previously described AMPs and were characterized by overrepresentation of hydrophobic residues and a low net positive charge. The identified peptides were confirmed as being able to enter Chinese hamster ovary cells in *in vivo* experiments. This type of screening illustrates that screening peptides in a simplified vesicle system is a viable route to the identification of novel AMPs with particular properties

Ultimately high throughput screening will be important for both the discovery of novel antimicrobial peptides from random or semi-random peptide libraries as well as for systematic analysis of the properties that confer antimicrobial activity in a small peptide. Analysis of large libraries may also be able to shed light on the properties that determine the mechanism of peptides and ultimately lead to the ability to rationally design peptides with desired therapeutic functions.

1.8 Goals of This Thesis

This thesis will address the issue of antimicrobial peptide design and mechanism study from two perspectives. Firstly it will explore the utility of histones as source material for antimicrobial peptide design through the characterization and analysis of three previously described novel histone derived antimicrobial peptides[23]. This type of study can illuminate AMP properties that contribute to antibacterial activity and determine a peptide's mechanism of action. In an effort to enable the further exploration of histone fragments with antimicrobial activity, this paper will also report efforts toward the establishment high-throughput techniques capable of identifying peptides with antimicrobial activity and providing preliminary mechanistic information. Such screens would enable rapid screening of large libraries of histone fragments and easy identification of peptides warranting further detailed research. Ultimately both the knowledge of peptide mechanisms provided by detailed study and the identification efforts made possible through high-throughput screening will be necessary for the continued understanding and development of antimicrobial peptides as novel therapeutic agents to combat emerging and evolving infectious agents.

2. MATERIALS AND METHODS

2.1 Peptides

Buforin II F10W, Magainin 2, DesHDAP1, DesHDAP2, and DesHDAP3 were synthesized and purified by GenScript (Piscataway, NJ) to > 95% purity. Proline to alanine mutant versions of each designed peptide as well as peptides with an N-terminal biotin group were also obtained at > 95% purity. All peptides had an unmodified C-terminus with a free carboxylic acid, and peptides that did not have an N-terminal biotin group had a free amine group at the N-terminus with no other modification. Peptides were dissolved in nanopure H_2O and stored at − 20 °C. Peptide concentrations were determined from the absorbance signals of native tryptophan residues at 280 nm. Absorbance was measured with a Biorad SmartSpec Plus spectrophotometer (Philadelphia, PA) or a Thermo Scientific Nanodrop 2000 (Wilmington, DE).

2.2 Relationship between Colony-Forming units and Optical Density

A bacterial colony was picked from frozen stock and grown in Luria broth (LB) (20% LB w/v, Sigma, St. Louis, MO) overnight. The overnight culture was diluted 1:500 into new LB medium and allowed to grow to an optical density of between 0.2 and 0.5. The solution was serially diluted in LB media, and 100 μL aliquots of the $1:10^4$, $1:10^5$, and $1:10^6$ dilutions were

Table 1: Conversion factors used for calculations of bacterial concentration in solution.

Species Name	Catalog Number	OD600 conversion factor
Escherichia coli	ATCC #29212	2.5×10^8
Staphylococcus aureus	Carolina #155554A	3.66×10^8
Serratia marcesans	Carolina #155450A	2.58×10^8
Bacillus subtilis	ATCC #6051	8.76×10^7
Enterococcus faecalis	ATCC #29212	1.11×10^8

plated on LB agar (20 % LB w/v, 10% bacto agar w/v, Sigma, St Louis, MO). The plates were incubated overnight at 37^{o}C, then colonies were counted and used to determine the relationship between optical density and colony-forming units per mL. CFU conversion factors found in this manner were used for all subsequent evaluations of bacterial concentrations.

2.3 Radial Diffusion Assay for Peptide Activity

A bacterial colony was picked from frozen stock and grown in tryptic soy broth (TSB) (30% TSB w/v) overnight. The overnight culture was diluted 1:500 into new TSB medium and allowed to grow for an additional 2.5 hours. The bacterial suspension was pelleted by centrifugation at approximately 880 x g, resuspended in sterile phosphate buffer (10 mM sodium phosphate, pH 7.4), and pelleted again. The resulting pellet was resuspended in phosphate buffer, and the concentration in colony-forming units per milliliter was determined as using the conversion factors found above (table 1). Underlay agar (9.1 mM phosphate, 10 g/L agarose, 0.27 g/L TSB medium, pH 7.4) was melted in the microwave then allowed to cool to 42^{o}C. 4 x 10^{6} CFU of bacteria in solution were added to 10mL of molten agar, vortexed, poured into a 15 x 1000 mm petri dish, and allowed to solidify at room temperature. A Pasteur pipette attached to a vacuum line via a bleach trap was used to create wells in the agar. The wells were filled with 2.5 μL of 3 x 10^{-4} M peptide solution. The plates were then incubated at 37^{o}C for 3 hours, at which point 10 mL of molten overlay agar (60 g/L TSB, 10 g/L agarose) was added onto the underlay and allowed to cool. The plates were then incubated overnight at 37^{o}C and the diameter of bacterial clearance was measured under 7x magnification.

2.4 Absorbance Versus Time Profile

An *E. coli* colony was picked from frozen stock and grown in tryptic soy broth (TSB) (30 g/L TSB medium) overnight. The overnight culture was diluted 1:500 into new TSB medium and allowed to grow for an additional 2.5 hours. The bacterial suspension was pelleted by centrifugation at approximately 880 x g, resuspended in sterile phosphate buffer (10 mM sodium phosphate, pH 7.4), and pelleted again. The resulting pellet was resuspended in phosphate buffer, and the concentration in colony-forming units per milliliter was determined and adjusted to 5 x 10^6 CFU/mL in phosphate buffer. 150 μL of the bacterial solution was placed in the wells of a 96 well plate. Peptide was added to a final concentration of 10^{-4} M and the absorbance at 600 nm was monitored at 15 s intervals on a SpectraMax plate-reader (Molecular Devices, Sunnydale, CA). In order to assess cell viability during this procedure, 10 μL samples were removed from each well at appropriate time points, diluted 1:100 in TSB, and allowed to grow overnight on LB agar (20% LB w/v, 10% bacto agar w/v) at 37^{o}C.

2.5 Propidium Iodide Uptake Assay

E. coli picked from a frozen stock were allowed to grow overnight in TSB media (30g/L TSB medium). The overnight culture was diluted 1:500 into new TSB medium and allowed to grow for an additional 2.5 hours. The bacterial suspension was pelleted by centrifugation at approximately 880 x g, resuspended in sterile phosphate buffer (10 mM sodium phosphate, pH 7.4), pelleted again, and resuspended in sterile phosphate buffer to a final optical density of 0.5. Propidium iodide (PI) was added to a final concentration of 20 μg/mL and the system allowed to equilibrate. PI was excited at 535nm and fluorescence measured at 617nm on a Varian Cary

Eclipse fluorescence spectrophotometer (Agilent Technologies, Santa Clara, CA). After the cells had equilibrated, peptide was added to a final concentration of 2μM and PI fluorescence was monitored for the following 40 minutes. Increase in fluorescence due to peptide was determined by comparing the fluorescence 5 minutes after peptide addition to the averaged value for the fluorescence in the minute prior to peptide addition. Reported numbers represent the averages of at least 4 independent experiments.

2.6 Thiazole Orange Displacement Assay

A Varian Cary Eclipse fluorescence spectrophotometer (Agilent Technologies, Santa Clara, CA) was blanked with STE buffer (10 mM Tris, 50 mM NaCl, 1 mM EDTA, pH 8.0). A 1 mL mixture of dsDNA (1.10 μM base pair concentration) and thiazole orange (0.55 μM) was made in STE buffer. The dsDNA (IDT, Coralville, IA) used was derived from DNA adjacent to the histone H2A region identical to the BF2 sequence in a histone·DNA crystal structure (AAATACACTTTTGGT). Maximum fluorescence intensity was measured 5 min after DNA addition (excitation wavelength: 509 nm; emission wavelength: 527 nm). The solution was then titrated with successive additions of 78 μM peptide solution. The decrease in fluorescence was measured 5 min after each addition of peptide until the fluorescence intensity decreased to ~50% of the maximum fluorescence. The peptide concentration at which fluorescent intensity was decreased to half (C_{50}) was extrapolated using the linear fit function on Microsoft Excel. Reported measurements are from at least three independent experiments for each peptide.

2.7 LIVE/DEAD® Assay

The LIVE/DEAD® assay was performed according to manufacturer instructions provided by Invitrogen (Grand Island, NY). Briefly, *E. coli* were grown overnight in LB medium (20% LB w/v), diluted 1:1000 in LB, allowed to grow to mid-log phase, and pelleted by centrifugation at ~880 x g. Pelleted bacteria were resuspended in a small volume of sterile phosphate buffer (10 mM sodium phosphate, pH 7.4). The resuspended bacteria solution was split in half and incubated in either phosphate buffer or 70% ethanol for 1 hour at room temperature. After incubation, the bacteria were once again pelleted by centrifugation and resuspended in phosphate buffer. Optical density of each solution was measured and used to calculate bacterial concentration in colony forming units/mL, then solutions were adjusted to 1 x 10^8 CFU/mL. A standard curve was constructed by combining live and ethanol-killed bacteria in known ratios to a total volume of 100 μL in the wells of a 96 well plate or a total volume of 3 mL in a quartz cuvette. SYTO9 and propidium iodide dyes were combined and diluted to prepare a concentrated stain solution (2X for plate reader, 10x for fluorimeter), which was added to the bacterial solution for a final concentration of 5.01 μM SYTO9 and 30 μM propidium iodide. After dye addition, the solutions were incubated for 15 minutes at room temperature while protected from light. At this time the fluorescence spectra were measured using a SpectraMax M3 multi-mode microplate reader (Molecular Devices, Sunnyvale, CA) or Varian Cary Eclipse fluorescence spectrophotometer (Agilent Technologies, Santa Clara, CA). Both dyes were excited at 485 nm; SYTO9 fluorescence was measured at 530 nm and propidium iodide fluorescence was measured at 630 nm. The standard curve, created using a linear regression on Microsoft Excel, was used to establish a relationship between ratio of SYTO9/PI fluorescence and the % live cells.

In order to determine the viability of bacteria exposed to antibacterial agents, bacteria were grown, pelleted, incubated in phosphate buffer, quantified, and diluted to 1 x 10^8 CFU/mL as described above. 100 μL of the bacterial solutions were aliquoted into the wells of a 96 well plate, and appropriate peptide or antibiotic was added to a final concentration of 1 x 10^{-5} M. Bacteria were incubated with the peptide for 30 minutes at 37^{o}C. SYTO9 and propidium iodide dyes were combined and diluted to prepare a 2X stain solution (10.02 μM SYTO9, 60 μM PI). 100 μL of the stain solution was added the bacterial solution in the plates and incubated for 15 minutes at room temperature protected from light. At this time the fluorescence spectra were measured using a SpectraMax M3 multi-mode microplate reader (Molecular Devices, Sunnyvale, CA). Both dyes were excited at 485 nm; SYTO9 fluorescence was measured at 530 nm and propidium iodide fluorescence was measured at 630 nm.

2.9 Turbidity-based Antimicrobial Activity Assay

An *E. coli* colony was picked from frozen stock and grown in tryptic soy broth (TSB) (30 g/L TSB medium) overnight. The overnight culture was diluted 1:500 into new TSB medium and allowed to grow for an additional 2.5 hours. The bacterial suspension was pelleted by centrifugation at approximately 880 x g, resuspended in sterile phosphate buffer (10 mM sodium phosphate, pH 7.4), and pelleted again. The pellet was resuspended in sterile phosphate buffer, and the optical density at 600nm was used to determine the concentration of the solution. Bacteria were diluted to 1 x 10^3 CFU/mL in liquid testing medium (0.3 g/L TSB, 0.1M NaH_2PO_4, 0.15M NaCl, pH 7.25). 100 μL of this solution was placed in the wells of a 96 well plate, and treated with the appropriate concentration of peptide (final peptide concentrations tested ranged from 5 to 30 μM). Plates were covered tightly with plastic wrap to prevent

evaporation and incubated at 37°C for 3 hours. After this incubation, 100 μL of 2X TSB (60 g/L) was added to each well and the plates were re-covered and incubated at 37°C overnight. Wells were scored visually using a binary "growth"/"no growth" system after 14-17 hours of overnight growth.

2.10 Confocal Microscopy with LIVE/DEAD Dyes

Bacteria were grown, pelleted, and incubated in either phosphate buffer or 70% ethanol as described in the Live/Dead procedure. Bacterial solutions were incubated with staining solution (5.01 μM SYTO9, 30 μM propidium iodide) for 15 min at room temperature protected from light, then placed on a poly-L-lysine coated slide and observed under 1000X magnification using a Leica TCS-SP1 confocal microscope with excitation at 488 nm.

2.11 Lipid Vesicle Preparation and Quantification

Phospholipids dissolved in chloroform were purchased from Avanti Polar Lipids (Alabaster, AL). N_2 stream was used to evaporate the chloroform off of a mixture of phosphatidylcholine (PC): phosphatidylglycerol (PG) and the resulting lipid cakes were kept in a desiccator overnight. Anhydrous lipid cakes were rehydrated in appropriate solution and subjected to five freeze–thaw cycles. Vesicles were extruded 21 times through a nuclepore track etch membrane with 0.1 μm pores (Whatman, United Kingdom) in an Avanti Polar Lipids extruder at a temperature of ~40°C to ensure uniform vesicle size.

Vesicle concentration was measured in triplicate as a function of total phosphorus content in solution as described by Avanti (http://www.avantilipids.com/index.php?option=com_

content&view=article&id=1686&Itemid=405). Briefly, a standard curve was constructed by treating various volumes of 0.65 mM phosphorus (KH_2PO_4) solution with 450 μL of 8.9 N sulfuric acid prior to 25 minutes of baking at 180°C. At this point 150 μL of H_2O_2 was added and the solutions were baked at 180°C for an additional 30 min. The solutions were removed from the oven, and water, ammonium molybdate, and ascorbic acid were added. Solutions were boiled in a water bath, for 7 minutes, and absorbance was determined at 820 nm. The standard curve was determined using a linear fit on Microsoft Excel. The total phosphorous content of the extruded vesicle solution was determined by subjecting a small volume of vesicle solution to the same procedure described above for the standards. The standard curve was used to determine the total phosphorous content in the vesicle sample based on the absorbance.

2.12 Calcein Self-Quenching Assay for Permeabilization

Phospholipids dissolved in chloroform were purchased from Avanti Polar Lipids (Alabaster, AL). N_2 stream was used to evaporate the chloroform off of a 3:1 mixture of phosphatidylcholine (PC): phosphatidylglycerol (PG) and the resulting lipid cakes were kept in a desiccator overnight. Anhydrous lipid cakes were rehydrated in 50 mM calcein (Sigma, St. Louis, MO) in TES buffer (100 mM NaCl, 10 mM TES, 0.1 mM EDTA, pH 7.4), and vesicles were prepared and quantified as described above. Peptides were added to added to wells of a 96 well plate such that their final concentration in solution would be 6μM. Equivalent volumes of water and 10% Triton-X100 were used as negative and positive controls, respectively. Vesicles were diluted to a concentration of 3×10^{-5} M and 200 μL of the vesicle solution was added to the wells containing peptide. Fluorescence was monitored using a SpectraMax M3 multi-mode microplate reader (Molecular Devices, Sunnyvale, CA) (ex: 470 nm, em: 509 nm). Percent

permeabilization was determined according to the following formula, using water and triton-X treated wells as 0% and 100% respectively:

$$\% \text{ permeabilization} = \frac{(\text{peptide} - H_2O)}{10\% \text{ Triton-X} - H_2O} \times 100$$

2.13 Trypsin Digestion Translocation Assay

Phospholipids dissolved in chloroform were purchased from Avanti Polar Lipids (Alabaster, AL). N_2 stream was used to evaporate the chloroform off of a 50:45:5 mixture of phosphatidylcholine (PC): phosphatidylglycerol (PG): 5-dimethylaminonaphthalene-1-sulfonyl phosphatidylethanolamine (DNS-PE) and the resulting lipid cakes were kept in a desiccator overnight. Vesicles were rehydrated in a solution of 0.2 M porcine trypsin (Sigma Aldrich T-0303) in HEPES buffer (10 mM HEPES, 45 mM NaCl, 1 mM EDTA, pH 7.4) for the experimental condition or a solution of 0.2 M porcine trypsin and 2 M trypsin-chymotrypsin inhibitor (Sigma Aldrich T-9777) in HEPES buffer for the control condition. Vesicles were then prepared and quantified based on total phosphorous content as described above. Phosphorous content of control vesicles was blanked against a solution containing the equivalent volume of trypsin-chymotrypsin inhibitor but lacking any vesicles. Vesicles were diluted to a final concentration of 0.25 mM in a solution containing 10X molar equivalent of trypsin inhibitor as compared to the trypsin in the vesicle solution. Peptides were prepared at a concentration of 2.5 x 10^{-4} M in nanopure water and 2 μL of peptide solution was placed in each well of opaque 96 well plates (VWR, Radnor, PA). 200 μL of the vesicle-containing solution was added to each well and fluorescence monitoring begun immediately. Fluorescence was measured using a SpectraMax M3 multi-mode microplate reader (Molecular Devices, Sunnyvale, CA) using an

excitation of 280 nm and measuring emission at 525 nm. Fluorescence was monitored for 25 minutes, and percent decrease determined by dividing the average fluorescence in the final minute by the fluorescence at t = 0. Translocation ratio of the experimental sample relative to the control condition was determined using the following formula:

$$\text{Translocation ratio} = \frac{\frac{F_{control}\ \text{final minute}}{F_{control}\ \text{initial}}}{\frac{F_{exp}\ \text{final minute}}{F_{exp}\ \text{initial}}}$$

3. NOVEL HISTONE DERIVED ANTIMICROBIAL PEPTIDES

Previous work resulted in the successful design of three histone-derived antimicrobial peptides (HDAPs) based on the important properties of BF2[23]. Like BF2, each of the novel HDAPs was polycationic, amphipathic, and primarily helical with a single helix-breaking proline hinge (table 2). Each of the three novel HDAPs displayed antimicrobial activity against a variety of gram positive and gram-negative strains. Because the proline residue is known to play an important role in BF2's antimicrobial activity, proline-to-alanine mutants of each peptide were also synthesized and assessed.

Table 2: Sequences of buforin II, DesHDAP1, DesHDAP3, and DesHDAP3 with proline residues shown in red.

Peptide	**Histone Subunit Source**	**Amino Acid Sequence**	**# of Amino Acids**
Buforin II (BF2)	H2A	TRSSRAGLQW**P**VGRVHRLLRK	21
BF2 P11A	H2A	TRSSRAGLQW**A**VGRVHRLLRK	21
Magainin 2	-	GIGKFLHSAKKFGKAFVGEIMNS	23
DesHDAP1	H2A	ARDNKKTRIW**P**RHLQLAVRN	20
DesHDAP1 P11A mutant	H2A	ARDNKKTRIW**A**RHLQLAVRN	20
DesHDPA2	H3	HRYR**P**GTVALREIRRYQKST	20
DesHDAP2 P5A mutant	H3	HRYR**A**GTVALREIRRYQKST	20
DesHDAP3	H4	KVLRDNIQGWTK**P**AIRRLARRG	22
DesHDAP3 P13A mutant	H4	KVLRDNIQGWTK**A**AIRRLARRG	22

Interestingly DesHDAP1 was more potent than BF2 against *E. faecalis*, similarly potent against *E. coli* ATCC 29212, *S. marcesens*, and *B. subtilis*, and less potent than BF2 against *E. coli* Top10 and *S. aureus*[23]. Although differences in absolute potency were expected when peptides were applied to different bacterial strains, it would be predicted that the relative efficacies of the different peptides should be fairly consistent. That is, stronger peptides should always be more effective than weaker peptides regardless of bacterial strain. This is not the trend that was observed, and the origins of the species-dependent changes in relative efficacies remain unexplained. Notably the observed pattern does not correlate with gram-positive versus gram-negative bacteria as might be expected if the presence of a cell wall were responsible for these changes.

Bacterial populations in solution are often measured by observing the turbidity from intact bacteria scattering light. Previous studies have also used this phenomenon to characterize the effects of cytolytic agents because lysed bacterial cells fail to scatter light in a similar matter so the application of a cytolytic agent results in a rapid decrease in optical density[21]. When the lytic activities of the designed peptides were analyzed in this manner, DesHDAP1 demonstrated a profile similar to that of BF2, characterized by an increase in absorbance despite the fact that cells in solution have already become nonviable as measured by ability to grow overnight on agar plates. However both DesHDAP2 and 3 demonstrated profiles with the drop in absorbance characteristic of lysing cells. In order to understand these observations and evaluate whether the common features of the novel HDAP design were sufficient to confer peptides with a similar antimicrobial mechanism, we sought to characterize the antibacterial mechanisms of the novel DesHDAPs.

Because presence of the proline hinge is so critical to the function of BF2, each novel HDAP was also designed to include a single proline residue. In order to evaluate whether the proline plays a similar role in the antimicrobial mechanism of the novel HDAPs, the translocation, permeabilization, and overall antimicrobial abilities of the designed peptides were compared to the abilities of proline-to-alanine mutants.

3.1 Designed HDAPs do not share a mechanism of action

BF2's antimicrobial potency is dependent on its ability to cross bacterial and lipid vesicle membranes[32,58]. The absorbance profiles of bacteria exposed to DesHDAP1 resemble those of BF2, suggesting that it too might use a translocation-based antimicrobial mechanism[23]. In contrast, the absorbance profile of cells exposed to DesHDAP3 shows a dramatic drop in absorbance, signifying cell lysis. This effect suggests that, unlike DesHDAP1, DesHDAP3 may not share a mechanism with BF2. The designed peptides' translocation abilities into bacteria were assessed qualitatively using confocal laser microscopy. In these experiments, *E. coli* were exposed to biotinylated DesHDAP1 and DesHDAP3 and visualized with a streptavdin-AlexaFluor488 conjugate. Like BF2, DesHDAP1 generally appeared to be internalized by bacteria that showed fluorescence (figure 3A). In contrast, DesHDAP3 showed little entry into cells and was primarily localized to bacterial cell membranes (figure 3B).

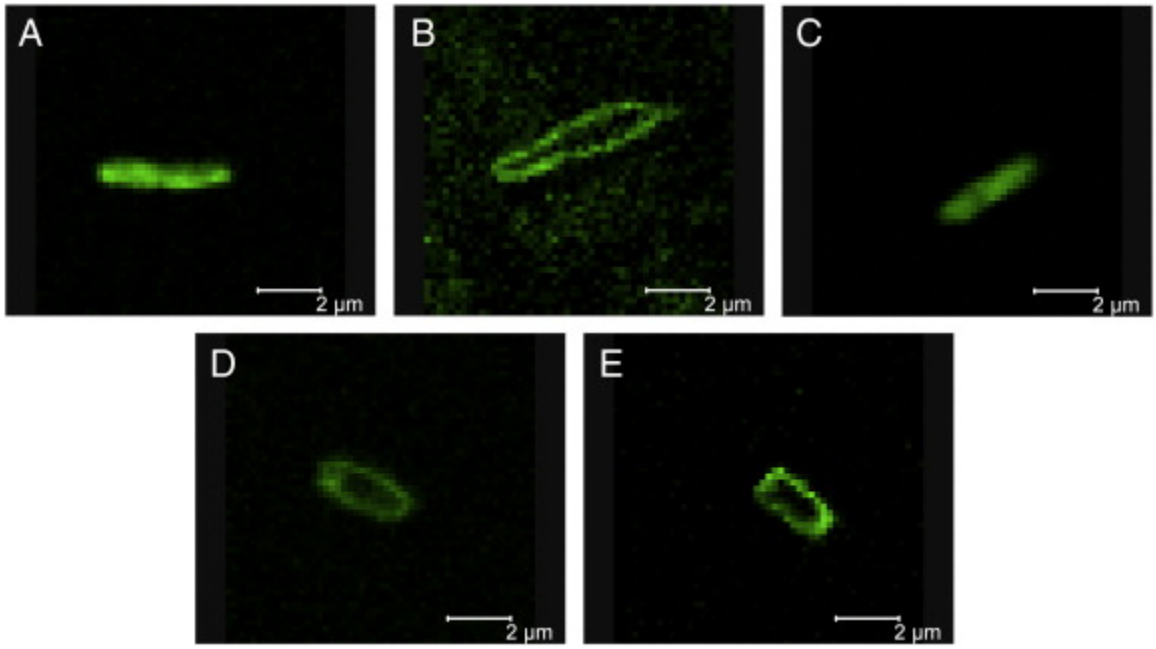

Figure 3. Localization of DesHDAP1 (**A**), DesHDAP3 (**B**), DesHDAP1 P11A (**C-D**), DesHDAP 3 P13A (**E**) into *E. coli*. 10^7 CFU/mL bacteria were incubated with biotinylated peptides (16 μg/mL). Peptides localization was assessed following treatment with a streptavidin-AlexaFluor488 conjugate and visualized on a Leica TCS-SP1 confocal microscope with excitation at 488 nm.

The designed HDAPs' translocation abilities were also assessed more quantitatively using the vesicle based translocation assay previously used by Matsuzaki and co-workers to characterize the function of BF2[59]. In this assay, the native tryptophan residues in each peptide act as FRET donors when associated with the dansylated lipids in the 50:45:5 POPC:POPG:DNS-POPE lipid vesicles, producing a fluorescent signal. As peptides cross the lipid bilayer, they are digested by trypsin trapped within the vesicle, leading to a loss of FRET signal. To control for loss of FRET signal due to incomplete inhibition of the trypsin outside vesicles or other factors unrelated to translocation ability, the FRET signal between the peptide and vesicles encapsulating both trypsin and trypsin inhibitor was also monitored. A significant

decrease in FRET signal as compared to the control is therefore indicative of a peptide that readily crosses membranes.

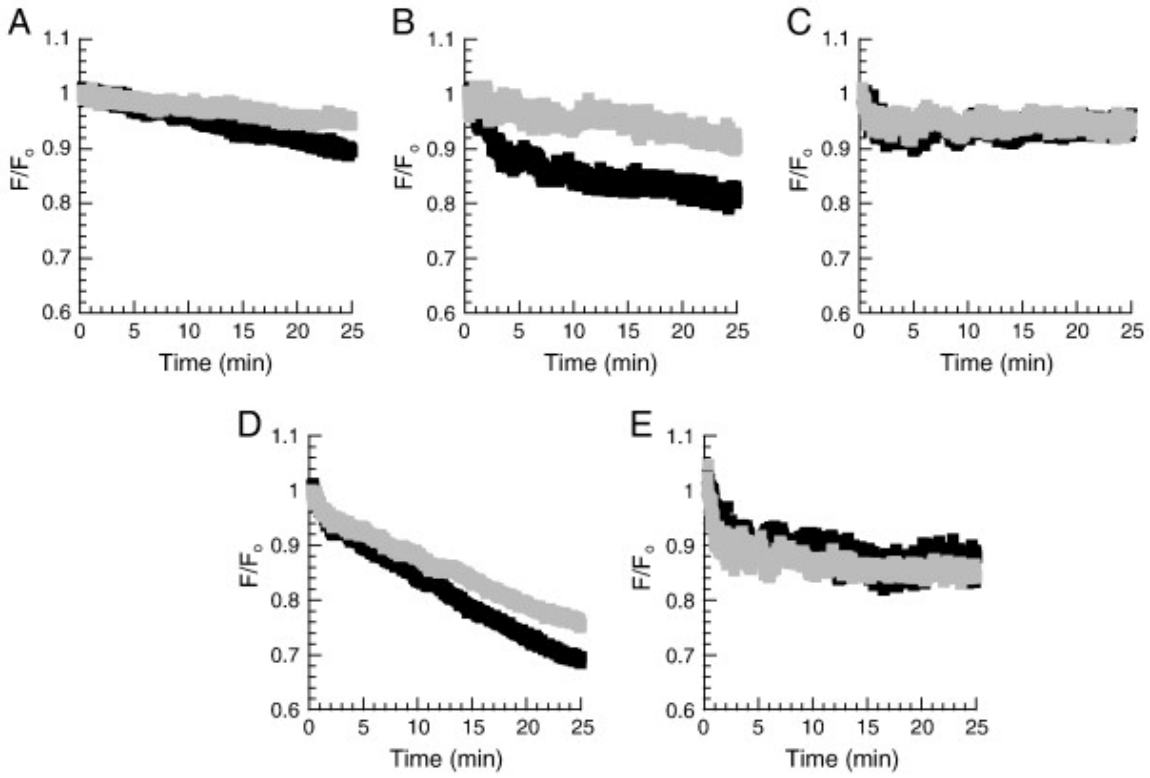

Figure 4. Translocation of BF2 (A), DesHDAP1 (B), DesHDAP3 (C), DesHDAP1 P11A (D), and DesHDAP3 P13A (E) across lipid vesicle membranes. Peptides (3 µM) were exposed to lipid vesicles (250 µM) containing trypsin. The FRET signal at 525 nm (black) is plotted as the fluorescent signal throughout the experiment relative to the initial fluorescent signal (F/F_o). In control traces (grey) peptides were exposed to vesicles containing both trypsin and trypsin inhibitor.

The drop in fluorescence observed for DesHDAP1 (figure 4B) is significantly greater than the drop observed in control vesicles containing inhibited trypsin. In our experience, the relative fluorescence drop observed for DesHDAP1 is even larger than that observed for BF2 in our vesicle samples (figure 4A). Together with the observed translocation into *E. coli* cells, this suggests that DesHDAP1, like BF2, is a cell-penetrating AMP that spontaneously crosses lipid membranes.

In order to quantify the translocation, we averaged the ratio of the control and experimental signals over three independent experiments. Our quantitative translocation ratio for BF2 is somewhat lower than the apparent value in data shown by Kobayashi et al[59]. This difference was likely due to the different sources of lipid (egg lipids versus chemically synthesized POPC and POPG used in this study) and different sources of trypsin and trypsin inhibitor. However, our quantitative translocation ratios for both BF2 and DesHDAP1 are indicative of membrane translocation. In contrast, DesHDAP3 showed a much smaller decrease in fluorescence when compared to controls (figure 4C), indicating that it did not exhibit appreciable translocation (Table 3).

Table 3. Translocation of DesHDAP1, DesHDAP3 and their proline to alanine mutants into lipid vesicles. The reported translocation ratios represent the ratio of the retention of fluorescence after 25 min of the translocation control to that of the experimental conditions. Uncertainty is reported as a standard deviation.

Peptide	Translocation ratio
DesHDAP1	1.13 ± 0.08
DesHDAP1 P11A	1.11 ± 0.01
DesHDAP3	0.97 ± 0.04
DesHDAP3 P13A	0.982 ± 0.005
Buforin II	1.07 ± 0.06

After translocating across the cell membrane, cell-penetrating AMPs must be able to reach and interact with their intracellular target(s). In BF2, DNA binding is correlated with overall potency, indicating that DNA binding is indeed critical to the bactericidal mechanism[34]. The DNA binding strength of DesHDAPs 1 and 3 was assessed by measuring the peptide concentration required to displace thiazole orange from double stranded DNA (Table 4). In this assay, DesHDAP1 bound DNA somewhat more weakly than BF2, which may partially explain

why BF2 is more potent against some bacterial strains than DesHDAP1[23]. In contrast, DesHDAP3 bound to DNA with approximately the same affinity as BF2. However, since DesHDAP3 is unable to cross membranes effectively, its enhanced DNA binding would be less relevant for its antimicrobial activity. Moreover, the differences in DNA binding between these peptides are relatively small and therefore likely less important in determining functional differences than the differing translocation and permeabilization abilities

Table 4. DNA binding of the novel HDAPs measured by fluorescent intercalator displacement. The concentration of peptide required to decrease the fluorescence of thiazole orange by 50% (C_{50}) was calculated by monitoring the decrease in fluorescence. Relative binding is normalized compared to BF2. Uncertainty is reported as a standard deviation.

Peptide	C_{50} (μM)	Relative C_{50}
BF2	8.0 ± 1	1
DesHDAP1	10.2 ± 0.5	1.28
DesHDAP3	8.7 ± 1	1.09

If DesHDAP3 does not function through effective translocation across lipid membranes, its antimicrobial activity may arise from an ability to permeabilize membranes. To test this possibility, we measured membrane permeabilization with a propidium iodide (PI) based assay. PI is a membrane-impermeable DNA intercalator, so fluorescence is indicative of membranes that have been disrupted. Although these peptides do have some affinity for DNA, appreciable competition between peptide and PI binding should not occur because of the high DNA binding constant of PI and the 750-fold higher concentration of PI compared to peptide in these experiments. Both designed peptides were relatively unable to permeabilize *E. coli* membranes (Table 5), showing a lower fluorescence from PI entering the cell than observed for BF2. The observations that DesHDAP3 is less effective at membrane translocation and no better at causing

membrane permeabilization than DesHDAP1 are consistent with the relatively lower antibacterial activity of the wild type DesHDAP3 peptide.

Table 5. The effect of proline-to-alanine mutations on the permeabilizing ability of DesHDAP1 and DesHDAP3. Propidium iodide, a membrane impermeable DNA intercalator, can enter bacterial cells only after membrane disruption. Data is presented as the ratio of propidium iodide fluorescence at 617 nm 5 min after addition of 2 μM peptide to the fluorescence before peptide addition. Uncertainty is reported as standard deviation.

	F_5/ F_0	
	Wildtype	Proline mutant
BF2	1.29 ± 0.1	-
Magainin	1.52 ± 0.2	-
DesHDAP1	1.12 ± 0.06	1.06 ± 0.05
DesHDAP3	1.13 ± 0.08	1.57 ± 0.4

3.2 The proline hinge plays a different role in the function of DesHDAPs1 and 3

DNA binding and translocation studies indicate that DesHDAP1 likely uses a mechanism similar to the one employed by BF2, while DesHDAP3 is significantly less able to translocate across membranes. Both BF2's translocation ability and ultimately its bactericidal activity are closely tied to the presence of a helix-breaking proline hinge in its structure[32,58], as mutating this proline to alanine significantly decreases the antimicrobial potency and translocation ability of BF2 while increasing its membrane permeabilization[58,59]. Both DesHDAP1 and DesHDAP3 were designed to have an analogous proline hinge, so proline to alanine mutants of DesHDAPs 1 and 3 were generated to assess the role that the proline hinge plays in determining the mechanism and biological activity of these novel HDAPs.

CD spectra of the peptides in a solution of 50% trifluoroethanol confirm the structural changes that result from the proline to alanine mutations (figure 5). As observed previously[23], the wild type DesHDAP1 peptide has a CD spectrum very similar to that of BF2, implying that it likely shares a partially helical structure with BF2, whereas wild type DesHDAP3 has significantly greater helical character. As expected, the proline mutation increases the α-helical structure of both peptides. However, the effect is more dramatic for the DesHDAP1 peptide, which was originally less helical.

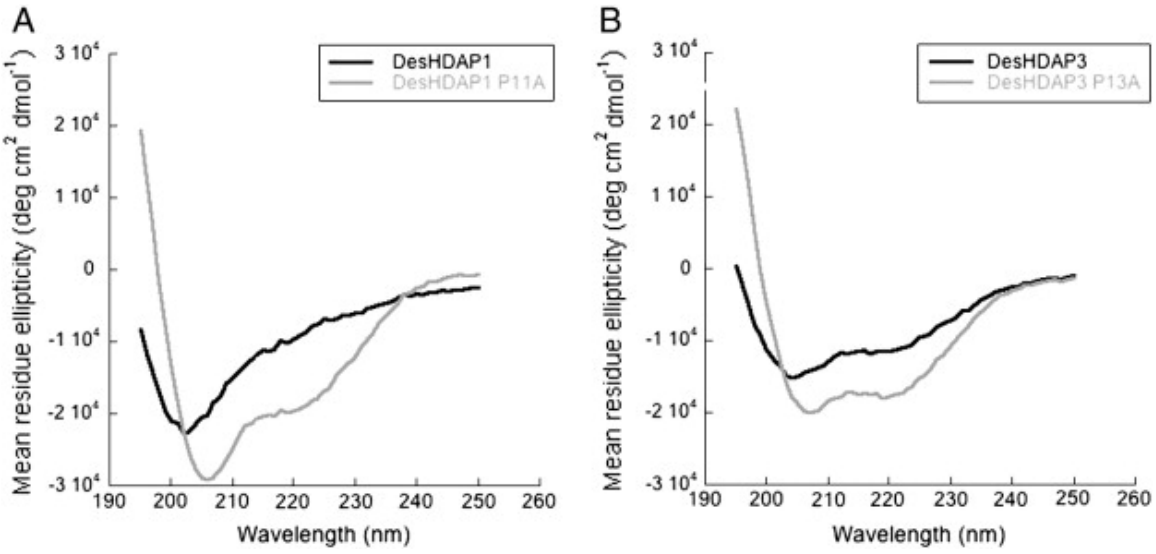

Figure 5. Circular dichroism spectra of all peptides were taken in 50% trifluoroethanol: 50% phosphate buffer solutions. A. CD spectra of DesHDAPs1 (black) and DesHDAP1 P11A (gray). B. CD spectra of DesHDAP3 (black) and DesHDAP3 P13A (gray)

Antibacterial potency of the DesHDAP1 and DesHDAP3 peptides and their proline mutants was measured using a radial diffusion assay (figure 6). As seen in previous studies, DesHDAP1 showed antibacterial activity similar to that of BF2, while DesHDAP3 had somewhat lower activity[23]. Like BF2 P11A, DesHDAP1 P11A showed reduced activity against all bacterial species tested (figure 6A). In contrast, removing the proline hinge improved the

bactericidal activity of DesHDAP3, as DesHDAP3 P13A showed greater activity against all bacterial strains than the parent peptide (figure 6B). In fact, the potency of DesHDAP3 P13A is comparable to that of DesHDAP1 and BF2.

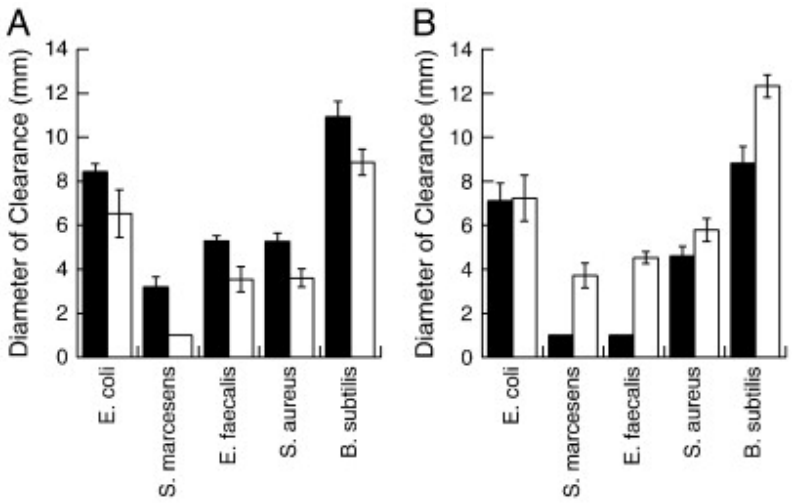

Figure 6. The antibacterial activity of the original DesHDAP1 (A) and DesHDAP3 (B) peptides (solid bars) and their respective proline-to-alanine mutants (white bars) were assessed with a radial diffusion assay. Error bars represent standard deviations.

In order to explain these divergent trends in activity for DesHDAPs 1 and 3, we characterized how the proline mutations altered the membrane translocation and permeabilization of the two peptides. The vesicle-based translocation assay suggested a slight decrease in DesHDAP1 P11A's translocation abilities compared with wildtype peptide (Table 3, figure 4D), although this decrease was within the experimental error of our method. Similarly, some bacteria exposed to DesHDAP1 P11A displayed peptide internalization, while others within the same slide showed localization of the peptide to the membrane (figure 3C-D). Together, these data suggest that the proline mutation may have reduced, but certainly did not eliminate, the efficiency of DesHDAP1 translocation. This reduction in translocation efficiency may explain the decrease in DesHDAP1 P11A bactericidal activity and suggests that the proline hinge plays a similarly important role in peptide translocation for both BF2 and DesHDAP1.

Like the wild type DesHDAP3, DesHDAP3 P13A showed minimal translocation in both lipid vesicle and bacterial studies (table 3, figure 3E, figure 4E). This suggests that the proline hinge greatly aids in translocation for some HDAPs, but that the proline hinge alone does not necessarily confer translocation abilities.

To assess whether any of the peptides might be working through a lytic mechanism rather than a cell-penetrating mechanism, membrane permeabilization in the presence of peptide was tested using the PI assay (Table 5). As shown above, both of the wild type DesHDAPs caused minimal membrane permeabilization. However, while DesHDAP1 P11A caused even less permeabilization than the wildtype designed peptide, DesHDAP3 P13A caused membrane permeabilization at a level comparable to magainin, a known lytic peptide[60]. Thus, it appears that the P13A mutation enhances the antibacterial activity of DesHDAP3 by converting the peptide into a much more effective membrane-permeabilizing agent.

3.3 Discussion

This work with novel HDAPs confirms that histones can serve as effective templates for antimicrobial peptide design. Their success also confirms that using features of known peptides to design novel AMPs is a viable strategy. However, despite the similar characteristics and design strategy, the three DesHDAPs discussed here do not share a mechanism of action, indicating that some additional property or properties are involved in the determination of antimicrobial mechanism. Interestingly the potency of these peptides does not correlate with their helical natures, suggesting that factors other than solely helical content must affect antibacterial activity.

Additionally, the proline hinge served to disrupt the alpha-helical nature of each peptide, but the effect of this disruption on antibacterial potency differed markedly. Notably DesHDAP1 became a weaker antimicrobial agent upon substitution of the proline residue with alanine because the peptide lost its ability to effectively cross lipid bilayers. In contrast neither DesHDAP3 nor its proline mutant were able to effectively cross lipid bilayers. Instead the increase in antibacterial activity upon proline-to-alanine substitution is likely a function of the increased ability of the DesHDAP3 P13A peptide to permeabilize cell membranes and therefore lyse bacteria.

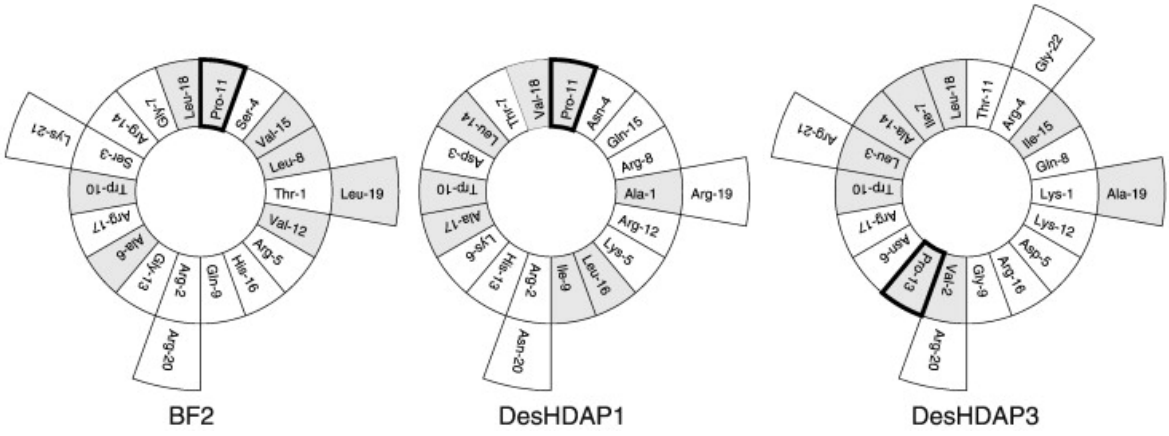

Figure 7: HDAP helical wheel depictions generated using the GROMACS suite. Hydrophobic residues are shown in grey, and the proline hinge is outlined.

DesHDAP3 has the most amphipathic character when in a fully helical conformation (figure 7), so seems plausible that the P13A mutation enhances antimicrobial activity because it allows the peptide to adopt a more ideal conformation for membrane interactions. Thus instead of using overall peptide helicity as a predictor of peptide potency, this study indicates that amphipathic character may be a more important determinant. For peptides such as DesHDAP3 that form highly amphipathic alpha helices, disruption of the helix by a proline residue is detrimental to the overall potency because of the subsequent reduction of amphipathicity. In

contrast peptides that form imperfectly amphipathic helices may benefit from proline disruption because the added flexibility allows the peptide to deform into a more amphipathic conformation.

It is also notable that the effect of the proline residue correlates so well with the predominant mechanism of action. It is plausible that the flexibility of a proline hinge is more important for peptides crossing all the way through a lipid bilayer than for peptides functioning through lytic mechanisms. Indeed, rigid helices might even be preferable if the predominant mode of antibacterial activity requires the formation of regular pores, as seen in the toroidal pore or barrel stave models of membrane lysis (figure 8) Indeed, this effect has been seen in several studies where the addition of a proline residue decreased the ability of peptides to disrupt cell membranes[61–63].

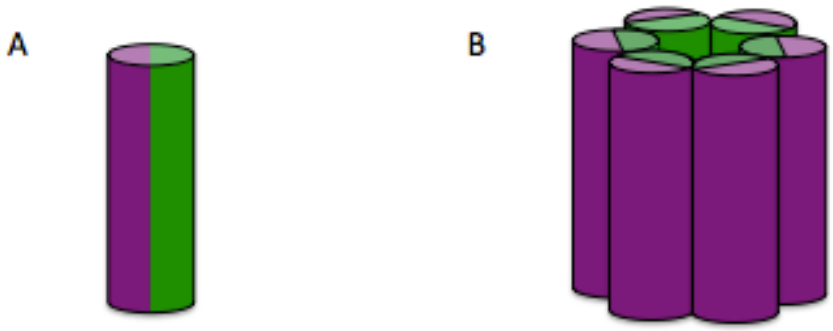

Figure 8: Amphipathic helices have segregated polar and nonpolar faces (A). Amphipathic helices are ideal for pore formation because the nonpolar surface forms and exterior that can interact with the nonpolar lipid tails of the membrane interior, while the polar face lines the inner aqueous pore (B).

Ultimately this study suggests that histones may be a fertile source of AMP template material but that histone homology alone does not predict a particular mechanism of action. In

order to further explore the determinants of HDAP potency and mechanism, it will be imperative to gather a larger set of characterized HDAPs.

4. DEVELOPMENT OF HIGH THROUGHPUT SCREENING

High throughput screening (HTS) techniques allow researchers to investigate the properties of many peptides at once and identify those that possess particular features. While it is important that HTS protocols are sensitive enough to distinguish peptides that possess desirable characteristics from those that lack them, these assays are intended for identification rather than exhaustive characterization and can therefore be less sensitive than other techniques. Peptides identified through HTS can be further characterized using the same techniques used to study other designed peptides. For our purposes, effective HTS protocols must be capable of identifying peptides with antibacterial activity and desirable mechanistic qualities. We are specifically interested in characterizing the antimicrobial mechanisms of AMPs, therefore it is important to know not only that a peptide is capable of killing bacteria but also whether it does so through membrane lysis or a translocation-based system. While antimicrobial activity screens must necessarily be done in vivo, both permeabilization and translocation can be addressed in a simplified vesicle system. Ideally, permeabilization and translocation could be assessed using the same vesicle population, thus further minimizing the volume of peptide required to gather this preliminary characterization.

4.1 Antibacterial activity

4.1.1 LIVE/DEAD® Bacterial Cell Viability Assay (Invitrogen)

Invitrogen's LIVE/DEAD® bacterial cell staining kit was used to assess the viability of bacterial cells after incubation with antimicrobial peptides. This procedure depends on monitoring the relative fluorescence from two DNA-intercalating dyes: SYTO9 and propidium iodide (PI). Both dyes are DNA intercalators, but differ in their binding affinity and ability to permeate bacterial cells. Propidium iodide is a well-characterized DNA-intercalator with a high

DNA affinity and fluorescence upon intercalation. However, propidium iodide is unable to cross intact cell membranes, a property which has led to its widespread utility in cell permeabilization assays[64–66]. In contrast SYTO9 is a fluorescent dye with a weaker DNA binding affinity, which is capable of crossing intact cell membranes[67–69]. Therefore when live bacteria with intact membranes are exposed to both dyes, only SYTO9 will be capable of accessing the DNA causing the cells to stain green. In contrast cells with disrupted membranes allow both PI and SYTO9 to enter the cell and compete for DNA binding[70]. Since PI has a higher DNA binding affinity it outcompetes SYTO9, staining these cells red. In order to create a standard curve for the percentage of living bacteria in a sample, bacteria are incubated in either phosphate buffer or 70% ethanol for one hour in order to create populations of live and dead bacteria, respectively. These live and dead populations are combined in known ratios and stained with the dye combination to create a standard curve.

Table 6: Representative LIVE/DEAD ratios from 9/30/12. Percent viability was calculated from the standard curve of ethanol-killed bacteria.

	Em 530	Em 630	ratio	% alive
H20	8877.8	865.1	10.3	120.2
Kan	5680.3	311.6	18.2	217.8
BF2	7417.5	594.1	12.5	147.5

For initial characterization of this assay for cell viability purposes, Kanamycin, a known and well-characterized antibiotic, was used at twice its minimum inhibitory concentration. The Invitrogen instructional manual suggests determining the percent viability using the ratio of fluorescence at 530 nm to fluorescence at 630 nm[70]. While this ratio produces an excellent standard curve for the combinations of live and ethanol-killed bacteria, the ratio suggested high cell viabilities for bacteria treated with antibacterial agents (table 6). Although the negative

control population treated only with water showed a fluorescence ratio comparable to the 100% live standard, bacteria treated with kanamycin consistently produced ratios suggesting greater than 100% viability (table 6). Further investigation revealed that these high ratios were a result of a dramatic decrease in propidium iodide fluorescence in these bacteria as compared to any of the other populations from the standard curve. In order to confirm that the laboratory stock of Kanamycin was indeed acting as an effective antibacterial agent, bacterial solution was removed immediately prior to staining, plated on LB agar, and allowed to grow overnight. These plates revealed that the kanamycin-treated cells were indeed non-viable by the time of the staining, while the control cells retained full replicative potential.

In order to obtain a more complete understanding of the fluorescent spectra from these stained bacterial populations, the fluorimeter was used to obtain the spectrum of sample fluorescence from 490 to 700 nm (figure 9). Although the kanamycin-treated bacteria retained a peak at approximately 510 nm that was also present in control bacteria, the fluorescence decreased dramatically at the higher wavelengths. Notably, the propidium iodide fluorescence in the 620-650 nm range was lower for the kanamycin-treated cells than for any of the standard conditions, including those with completely live bacteria where propidium iodide is considered to be completely excluded from cells.

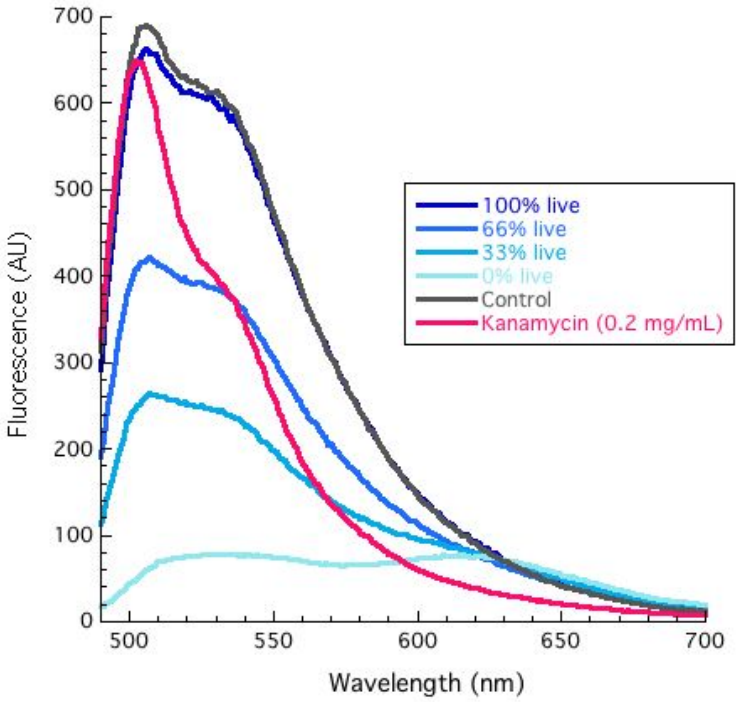

Figure 9: Fluorescence spectrum of 10^8 CFU/mL *E. coli* incubated with propidium iodide and SYTO9 dyes. Standardization solutions were prepared by combining ethanol-killed bacteria with bacteria incubated in buffer in appropriate ratios.

The observation that the PI fluorescence for kanamycin-treated cells is even lower than that observed from completely healthy cells with intact membranes suggested that there could be direct interactions between the antibiotic and the dye molecules. Kanamycin functions through ribosome inhibition and would therefore not be predicted to affect DNA intercalating behavior of either PI or SYTO9[64]. On the other hand, ribosomes contain significant portions of RNA[71] and ssDNA probes have been designed to detect the presence of kanamycin[72], suggesting that the antibiotic is capable of at least some forms of nucleotide interactions. While literature searches revealed no evidence of documented kanamycin-PI interaction, the existence of interactions that prevent PI from binding to DNA or that quench its fluorescence could explain the observed changes in fluorescence.

Confocal microscopy confirmed the spectroscopic observation that kanamycin-treated cells demonstrate robust SYTO9 staining at least comparable to that of live control cells (figure 10). However, kanamycin-treated *E. coli* were unable to grow overnight on LB agar, confirming that they were non-viable by the time of imaging. Because kanamycin functions through ribosome inhibition, it is possible that these cells could become non-viable significantly before the onset of any membrane deterioration.

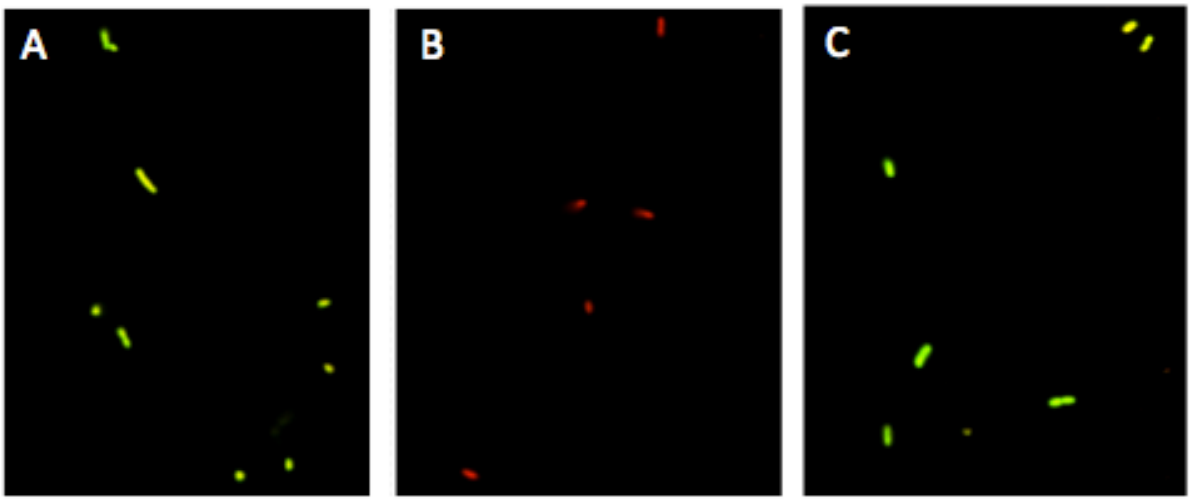

Figure 10: Confocal images of live (a) and ethanol-killed (b) *E. coli* demonstrate appropriate staining by live/dead dyes. Bacteria treated with 2 mg/mL kanamycin demonstrate robust Syto9 staining (c) but are non-viable.

In addition to the practical difficulties encountered during the attempt to implement this assay for antibacterial screening, some of the premises of the LIVE/DEAD® assay may argue against its appropriateness for use in antibacterial discovery. Firstly, the creation of the standard curve with live and killed bacteria assumes that a bacterial mixture can be adequately described with these binary states. In this model all cells that are alive are perfectly healthy and equivalent, while all dead cells are likewise completely permeable. This model has been used effectively for the characterization of mixed bacterial populations, such as biofilms, but is unlikely to accurately

portray the condition of bacteria exposed to antibacterial agents. Instead, bacteria exposed to antibacterial agents are likely to be unhealthy or physiologically stressed prior to complete cell death, states which this assay is not equipped to detect. Furthermore, the assay actually assesses membrane integrity rather than cells' ability to survive and reproduce. If the difficulties thus far observed are at least in part due to the fact that bacteria are being dyed after they have become non-viable but before the subsequent breakdown of membrane occurs, it follows that this assay might be more valid if the post-exposure window were lengthened. While the membranes of the non-viable bacteria observed here appear to remain largely intact up to 45 minutes after exposure to antimicrobial agents, it is possible that the same dying procedure applied after several hours might be able to identify bacteria which have begun to break down as a result of antimicrobial agent induced death. Although lengthening the timescale might allow this assay's use for antimicrobial screening purposes, the LIVE/DEAD® assay is not optimally designed for screening novel agents. Instead, research efforts were redirected toward identifying another, more appropriate assay.

4.1.2 Turbidity-Based Assay

Many antimicrobial screens use relatively simple assays for antibacterial activity that involve monitoring the turbidity of bacteria after an overnight incubation with the putative antibacterial agent[73,74]. While microbroth dilution assays vary the concentration of the antibacterial agent and are used to assess the minimum inhibitory concentrations of compounds known to have antimicrobial activity, a simpler assay can use untested compounds at some threshold concentration to assess whether or not they have appreciable antimicrobial activity warranting further study.

The initial antibacterial challenge is performed on bacteria in a nutrient poor testing medium in order to minimize bacterial growth during the exposure window and to eliminate the possibility of interactions between peptides and growth media. A 1 x 10^3 CFU/mL solution of log-phase bacteria in liquid testing media was added to wells of a 96-well plate containing an appropriate concentration of antibacterial agent and incubated for 3 hours at 37^{o}C. After this interval, a 2X nutrient broth was added and the plates were allowed to grow overnight. The following day wells were characterized using a binary growth/no-growth designation because all wells that demonstrated bacterial replication exhibited similar turbidity beyond the range quantifiable by a spectrophotometer. Quantitative characterization of turbidity would have been further inhibited by the heterogeneity of the bacterial suspensions; significant colonies of bacteria had settled to the bottom of the well because the overnight incubation did not include agitation. Because turbidity did conform well to a binary scoring system and there was good consistency between wells from the same treatment, this scoring system was deemed appropriate.

As with the previous assay of antibacterial activity, kanamycin (0.2 mg/mL) was used as a positive antibacterial control and an equal volume of sterile water as a negative control. While both positive and negative control wells displayed appropriate growth behaviors, neither buforin II nor DesHDAP1 caused any inhibition of cell growth at concentrations up to 30 μM (figure 11). Although a MIC has never been determined for DesHDAP1, literature values for BF2 MICs cite values of 2-4 μg/mL[13,32,58], or 0.8-1.6 μM. Although the peptides tested here demonstrate antimicrobial activity in an agar diffusion assay, indicating that they have not degraded, they are unable to inhibit growth in liquid medium even at concentrations approximately 10 times the published MIC.

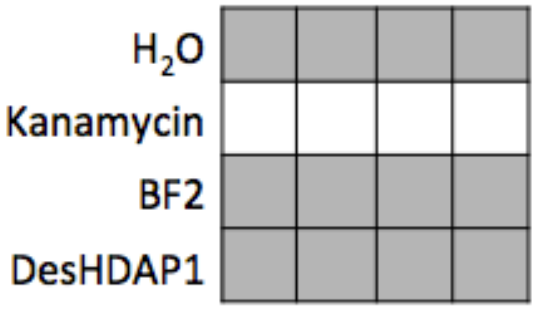

Figure 11: Overnight growth of E. coli after treatment with water, 2 mg/mL kanamycin, 30 µM BF2, or 20 µM DesHDAP1. Grey cells indicate significant bacterial growth in a well after 17 hours. Boxes in the same row represent replicates of a condition.

At present, we have no satisfactory explanation for this failure of BF2 to inhibit bacterial growth in solution. *E. coli* strain may play a role, as we used Top 10 while many of the studies cited previously use other strains. However, it seems unlikely that such large discrepancies in efficacy are due entirely to differences in laboratory strain susceptibility. At least one recent paper has reported a similar inability of BF2 to retard bacterial growth in solution. Lan et al observed that BF2 did not cause any growth inhibition of either Top 10 or NCTC9001 *E. coli* at peptide concentrations up to 26.30 µg/mL (10.8 µM), the highest concentration tested in their experiment[75]. However, they fail to provide any explanation for this anomaly, incorrectly citing differences in technique as the likely source of this disagreement. Despite the lack of satisfactory explanation, this seems to be evidence of a similar problem in the hands of other investigators. Performing this assay with other well-characterized AMPs would provide further evidence regarding whether the observed issues derive from the activity of BF2 itself or from the assay protocol used in our lab.

4.2 Membrane Permeabilization

4.2.1 Calcein Leakage

Calcein is a fluorescent dye often used for cell staining and for interrogation of vesicle volume and dynamics. Calcein is a particularly useful because it exhibits strong self-quenching

behavior at concentrations above 4 mM[76]. While the mechanism of this self-quenching is not entirely understood, it appears to result from dimerization into a non-fluorescent form coupled with energy transfer from monomers to dimers[77]. Because of this property, calcein and similar molecules are often used for investigation of vesicle volumes, fusion, or leakage.

Düzgüneş et al describes a dye leakage assay performed by encapsulating calcein at 35 mM within phospholipid vesicles and monitoring for an increase in fluorescence upon membrane disruption and subsequent release of calcein into the extravesicular solution[78]. After usual vesicle preparation in a solution of concentrated calcein and extrusion, the vesicle solution was purified on a gel-filtration column in order to separate the vesicles from the extravesicular calcein in the solution. The color of calcein solutions made this process particularly easy because it was possible to identify vesicle fractions by their characteristic orange color while unencapsulated calcein had a lighter fluorescent green appearance.

Positive and negative vesicle lysis controls were established by incubating the vesicles with 2 μL of Triton-X or ddH_2O, respectively. Both 1% and 10% V/V Triton-X100 were used in our trials because some initial data suggested that magainin showed an intermediate permeabilization level compared to 10% Triton-X100 but was indistinguishable from permeabilization caused by 1% Triton-X100. Ultimately this appears not to be the case (Table 5) because both concentrations are well above the critical micelle concentration for Triton-X100[78] and subsequent trials were approximately as consistent between detergent concentrations as within trials of the same detergent concentration.

Table 7: Percent permeabilization of calcein-containing vesicles as determined by comparing the difference in fluorescence between wells treated with peptide and those treated with water control to the difference in fluorescence between wells treated with Triton-X100 and those treated with water control. Wells from the same experiment are depicted in the same row.

	Date	Magainin	Buforin 2	Des3 P13A	Hipposin P26A	Hipposin P26A/P48A
1% Triton-X100	Jan 24	91.6	-38.2			
	Jan 24	110.3	-33.2	6.9		
10% Triton-X100	Jan 17	43.9	-27.7			
	Jan 29	105.9	-0.5	-30.1	23.4	-37.4
	Jan 29	111.3	-24.7	-18.9	25.2	9.8

Ten minutes of treatment with 6 μM magainin caused an increase in fluorescence from the vesicle solution comparable to that caused by detergent above the critical micelle concentration. In contrast, vesicles exposed to 6 μM buforin II consistently exhibited less fluorescence than vesicles treated with only water (figure 12). Both magainin and buforin, for which the most trials were conducted, produced at least one significant outlier. This makes it difficult to confidently interpret the single or even duplicate values collected for Des3P13A and Hipposin P26A and P26A/P48A.

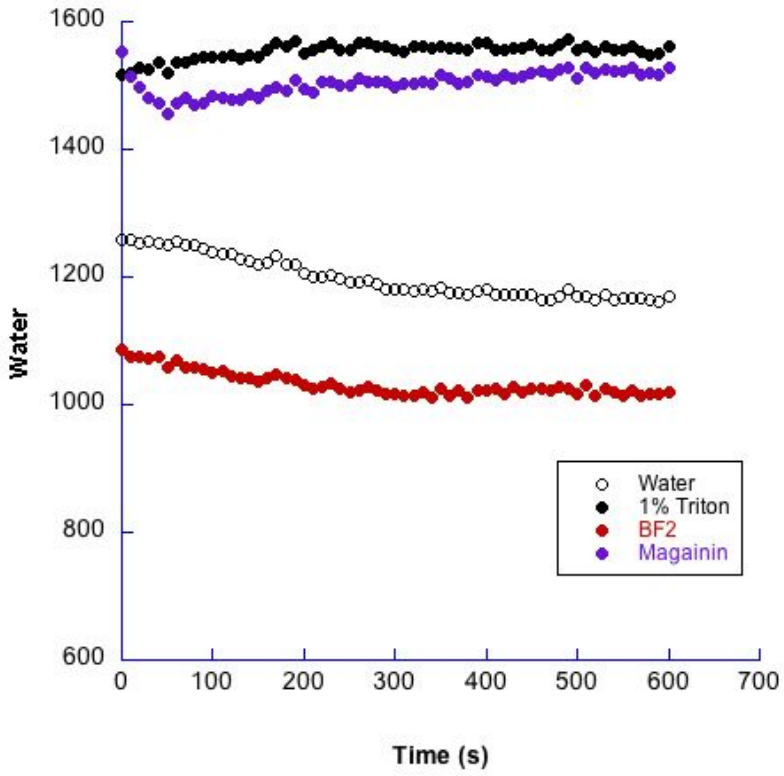

Figure 12: Representative plot of calcein fluorescence after vesicle treatment with peptide. PC/PG vesicles encapsulating 35 mM calcein were treated with 6µM peptide or equivalent volume of water. While magainin treatment caused an increase in calcein fluorescence, BF2 caused a decrease in fluorescence to a level below that of vesicles exposed only to water.

The outlying datapoints are less fundamentally concerning than the presence of negative percent permeabilization values. Based solely on the principles of self-quenching, there should be no mechanism for a peptide to decrease the level of fluorescence. Instead the observed decrease must be due to previously unconsidered factors, such as direct interactions between the peptides and the calcein molecules. Because calcein is anionic and our AMPs are polycationic, it would not be surprising to observe charge-based interactions between the two. The fluorescence (and solubility) of calcein itself is strongly pH dependent[79], so charge-based interactions with cationic peptides could significantly affect the dye's fluorescent behavior as well.

Furthermore, there is some research suggesting that the presence of surfactants such as triton, sodium dodecyl sulfate (SDS), or cetyltrimethylammonium bromide (CTAB) can affect the fluorescence behavior of calcein[80]. Interestingly the surfactants found to affect calcein fluorescence encompass diverse charges, including surfactants that are positively and negatively charged (CTAB and SDS respectively), as well as nonionic (triton). Specifically, Triton-X100 at concentrations greater than the critical micelle concentration significantly affected the fluorescence spectrum of calcein in HEPES, although the direction of the effect (enhancement or suppression of fluorescence) were inconsistent depending on the calcein concentration. This suggests that quantitative permeabilization assays using calcein may also suffer from interactions between the dye and surfactants used to obtain the 100% permeabilization positive control as well as from interactions between peptides and dyes.

Ultimately the potential for interactions other than self-quenching means that calcein-based assays will not provide reliable evidence of membrane permeabilization for antimicrobial peptide screens. While a self-quenching dye with less potential for intermolecular interactions with AMPs might accomplish the task, we elected to pursue other permeabilization protocols based on those that have been used successfully by other groups for similar assessments of peptide permeabilization.

4.2.2 Tb^{3+}/DPA Fluorescence

Previous high-throughput vesicle analyses of permeabilization and translocation have utilized the interaction between terbium III and dipicolinic acid (DPA) to assess vesicle lysis[57]. In this assay terbium (III) is encapsulated within lipid vesicles and extravesicular terbium is removed by size exclusion chromatography. DPA is then added to the vesicle solution, but is

unable to interact with the terbium because it cannot cross intact lipid bilayers. Upon addition of a membrane-permeabilizing peptide, vesicles will release Tb^{3+} into the surrounding solution where it will interact with the DPA and produce a robust fluorescent signal more than 1000 times greater than the signal from unchelated terbium ions[81]. This phenomenon is observed as a significant increase in fluorescence intensity when 50 mM DPA is introduced to a solution of 25 mM Tb^{3+} in HEPES (Figure 13).

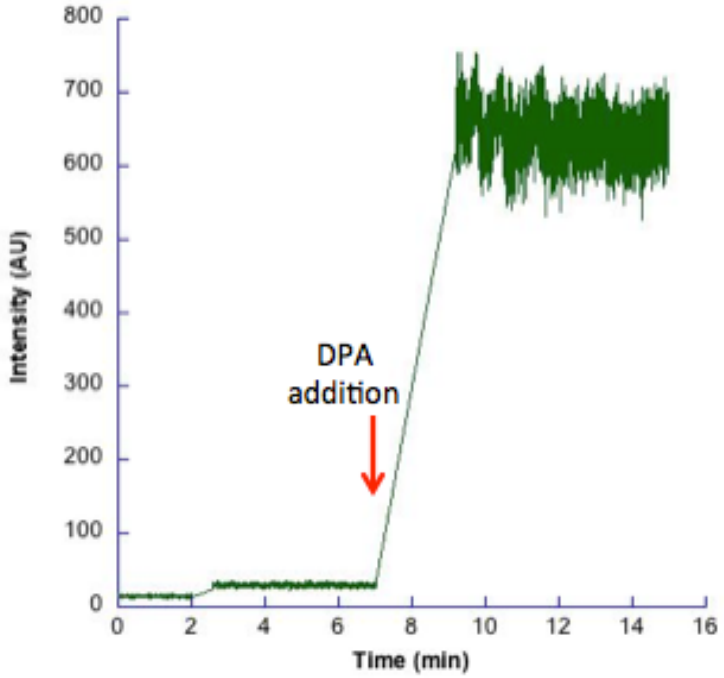

Figure 13: Fluorescence of 50 mM Terbium (III) in HEPES before and after the addition of 25 mM DPA.

The Tb^{3+}/DPA assay has several difficulties compared to the calcein-based assessment of permeabilization. Although it does not directly affect ease of performing the assay, Tb^{3+} is a heavy metal whose use requires appropriate waste disposal and management of contaminated materials. Additionally in our hands the inclusion of Tb^{3+} has seemed to exacerbate common problems with vesicle preparation, particularly difficulty extruding the vesicles through the membrane. Finally Tb^{3+} is colorless in solution, making the progression of vesicles and terbium

through the size exclusion column much more difficult to monitor compared to the similar process with colored calcein vesicles. Indeed we have not yet completed the successful preparation of vesicles in order to examine the utility of this assay for peptide assessment. However, its previous use in similar screens suggests that further manipulations could lead to the adaptation of this assay for effective permeabilization studies.

4.3 *Trypsin Digestion Translocation Assay*

Peptides that do not exert their antimicrobial activity through membrane permeabilization must be able to cross the lipid bilayer in order to interact with or inhibit intracellular components. A variety of monitoring techniques have been developed to assess peptide translocation. While confocal microscopy using labeled peptides can provide qualitative evidence for translocation, many researchers have turned to lipid vesicles for quantitative translocation metrics[55–57,73]. Vesicle-based assays simplify the experimental system and ensure that any observed translocation activity is definitively the result of peptide-lipid interaction.

Previous work in the Elmore lab has used a FRET-based trypsin degradation assay to observe the entry of the novel HDAPs into vesicles[82]. In this assay vesicles are prepared with 5% dansylated phosphatidylethanolamine (DNS-PE), which can undergo fluorescence resonance energy transfer (FRET) with tryptophan residues in membrane- associated peptides to produce a fluorescent signal[59]. These vesicles are reconstituted in a solution containing the proteolytic enzyme trypsin. After vesicle preparation and quantification, both the solution interior and exterior to the lipid vesicle contains trypsin. In order to prevent degradation of peptide in the extravesicular solution, a trypsin-chymotrypsin inhibitor is added at 10x the concentration of the

trypsin itself. Because the vesicles have already been formed, the inhibitor protein is unable to enter the vesicles and the interior trypsin remains uninhibited (figure 14)

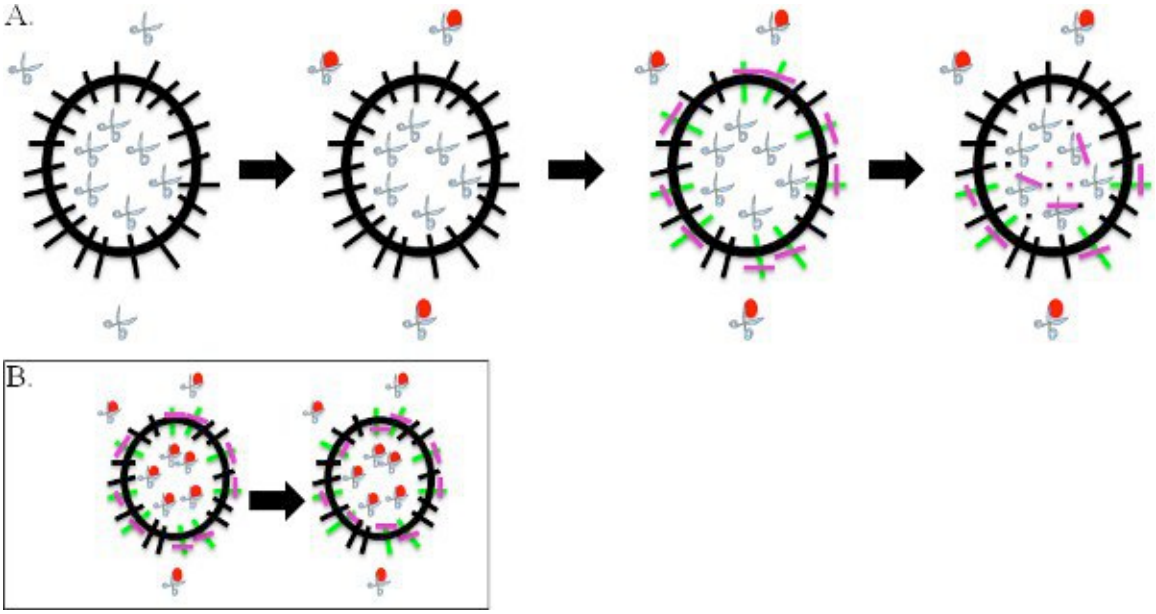

Figure 14: Schematic of translocation assay. Experimental LUV samples are doped with fluorescent dansyl POPE (black bars) and contain encapsulated trypsin (scissors) (A). Trypsin inhibitor (red circle) is used to inhibit trypsin outside the LUVs. The LUVs are exposed to peptide (purple). Peptide association with LUV membranes yields a FRET signal (green) that decreases as translocating peptides encounter uninhibited internal trypsin. Both trypsin and trypsin inhibitor are encapsulated in control LUV samples to measure decreases in FRET signal unrelated to translocation **(**B). [82]

Upon addition of peptide to the vesicle solution, the peptide associates with the lipid membrane and a FRET signal is measured. As translocating peptides cross the membrane they encounter the uninhibited trypsin, which cleaves the peptides after lysine or arginine residues. These degraded peptide fragments can no longer associate with the lipid bilayer, resulting in a loss of fluorescence signal. Therefore a decrease in fluorescence as the experiment progresses is indicative of a peptide that is effectively crossing lipid bilayers.

Because trypsin inhibition is incomplete even with the presence of excess inhibitor, it has proven essential to compare experimental trypsin degradation to that from vesicles where

intravesicular trypsin has also been inhibited. These control vesicles are rehydrated in a solution containing both trypsin and trypsin-chymotrypsin inhibitor (figure 14B). When peptide is added to these vesicles it can cross the lipid bilayer and enter the vesicles, but the inhibited trypsin will be incapable of cleaving the peptides. The peptides will therefore remain associated with the lipid membrane and continue to produce a detectable FRET signal.

Because the inhibitor can affect absolute fluorescence values, it is most illustrative to normalize both experimental and control fluorescence values against the initial value shortly after peptide addition. In this way degradation is seen as a percent decrease compared to the initial fluorescence rather than an absolute value. The difference between the decrease observed from experimental and control conditions illustrates whether or not peptides are effectively crossing the lipid bilayer.

Initial results using the plate reader to execute this assay suggest that this platform is both effective and capable of detecting similar values as compared to the fluorimeter. Notably peptides such as BF2 and DesHDAP1, which have been shown to translocate effectively by both the fluorimeter version of this assay and confocal microscopy (figures 3 and 4), show a clear distinction between the control and experimental conditions (figure 15). Furthermore the quantitative values obtained by comparing the fluorescence in the last minute of a 25 minute observation to the initial fluorescence produces a ratio similar to that described using the fluorimeter (table 8). Additionally peptides such as Des3 P13A, which do not translocate, produce similar levels of fluorescence in the control and experimental conditions, although the noise in this trial prohibited quantitative analysis. While these results have not yet been replicated, this initial success suggests that the volume and instrumentation will not present obstacles to high throughput usage of this assay.

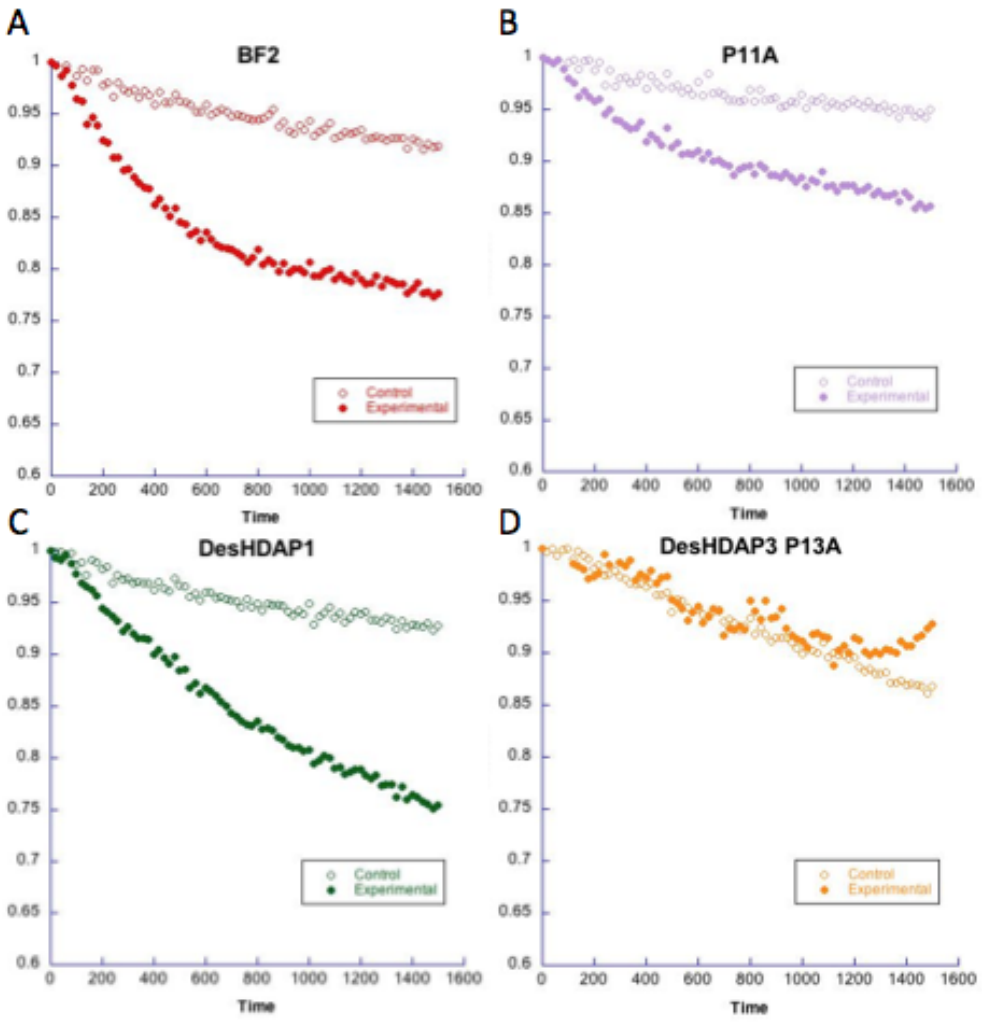

Figure 15: Translocation of peptides into lipid vesicles. Peptide translocation as measured by fluorescence decrease upon entry into trypsin-containing vesicles (solid circles) as compared to vesicles containing inhibited trypsin (open circles).

Table 8: Translocation ratios as measured on plate reader and fluorimeter. The reported translocation ratios represent the ratio of the retention of fluorescence after 25 min of the translocation control to that of the experimental conditions. Uncertainty is reported as a standard deviation.

Peptide	Plate reader ratio	Fluorimeter ratio (from table 3)
BF2	1.17 ± 0.02	1.07 ± 0.06
BF2 P11A	1.11 ± 0.006	-
Des1	1.19 ± 0.05	1.13 ± 0.08

The preparation and quantification of the vesicles for the translocation assay is both time consuming and difficult. Quantification of the phosphorus content in the control vesicles is particularly troublesome because the trypsin-chymotrypsin inhibitor is sold as a lyophilized powder in phosphate buffer. Thus the inhibitor solution adds additional phosphorus beyond that present from phospholipids in the vesicles. While it should be possible to use an appropriate volume of inhibitor solution to blank the quantification protocol for these vesicles, this has proven difficult. Specifically the samples containing the control vesicles have an absorbance very similar to the absorbance from the blank containing only inhibitor without any vesicles, making it difficult to accurately measure the lipid phosphorus content. Currently when such situations arise the concentration is assumed to be the same as the concentration of the experimental vesicles. However, because vesicles with inhibitor are typically much more difficult to extrude than those without, it seems likely that there are differences in final vesicle concentrations between the two samples. In the future in may be prudent to use dialysis to minimize or eliminate the phosphorus contribution of the inhibitor solution. However this buffer exchange could lead to a dilution of the inhibitor itself, making it more difficult to achieve the desired 1:10 trypsin: inhibitor ratio.

A second concern about this assay involves the time delay between peptide addition and the onset of fluorescent monitoring. Because of the difficulties in vesicle preparation, there is insufficient solution for the usage of a multi-channel pipette. The necessity of adding vesicle to solution to each well, changing tips, and inserting the plate into the fluorimeter means that the "initial" reading recorded by the instrument does not in fact represent the maximum prior to any trypsin digestion. This would artificially deflate the apparent translocation, since the apparent initial value would be measured after some degradation. However, the fact that we do see

continued digestion over the course of our monitoring and that this value is quantitatively similar to fluorimetry suggest that the assay remains viable. Greater familiarity with the plate reader and strategic positioning of experimental wells could likely decrease, though not eliminate, this lag.

5. FUTURE DIRECTIONS

5.1 Antibacterial Activity:

Previous characterizations of peptide efficacy in the Elmore lab have been performed using agar-based radial diffusion assays (RDAs) because they are easy to read, require little peptide, and give excellent data regarding the relative strengths of tested peptides. However it is difficult to extract quantitative information about inhibitory concentrations from RDAs because the diffusion of the peptide solution away from the well results in a logarithmic relationship between concentration and distance from the well. On a more fundamental level, the RDA does not test antimicrobial activity in a way that is reminiscent of the conditions that would be encountered *in vivo*. Bacteria suspended in the agarose medium are forced to grow in physiologically unnatural and primarily anaerobic conditions, which could affect their response to antimicrobial agents. In addition, the agarose gel itself might affect peptide properties or interact directly with the peptides. For these reasons, antimicrobial activity assessments performed in liquid medium likely provide a more valid measurement of true AMP potency.

Turbidity based activity screening is straightforward, widely used in drug discovery, and not demanding in reagents, time, or technology. Based on these criteria such assays should be ideally suited to high-throughput activity screens in Wellesley laboratories. However, while both the positive and negative controls demonstrate appropriate growth conditions in this assay, none of the antimicrobial peptides tested inhibited bacterial growth at concentrations up to 30 μM. This is nearly 10x greater than the published MIC for BF2[13], though the laboratory stock of peptide is has been confirmed as an active antimicrobial agent in RDA measurements, indicating that it has not degraded.

Unfortunately, the simplicity of the turbidity screening assay makes it particularly difficult to identify potential sources of error. Attempts to more closely mimic the conditions used in successful literature applications may help through optimizing bacterial growth conditions or eliminating unforeseen inhibitory effects. While the low MIC's generally acknowledged for BF2 have been widely replicated, the one paper reporting similar troubles observing inhibition from BF2[75] could represent another valuable source for identifying any factors contributing to our seemingly anomalous results.

Alternately, there are some bacterial cell viability assays that measure cell death through other mechanisms. Metabolic assays present one such promising avenue. Much like the MTT assay commonly used to assess eukaryotic cell viability[83], these assays measure bacterial health based either on the presence of key metabolic components or on the ability of living cells to metabolize one compound into a spectroscopically distinct metabolite. For example, the BacTiter-Glo™ system from Promega measures metabolically active cells through quantification of ATP levels, while carboxyfluorescien and related compounds are cleaved by esterases to produce fluorescent products, and rhodamine 123 staining identifies cells capable of maintaining appropriate cell potential[84]. These physiological state probes may be capable of identifying bacterial responses to peptide treatment on a more relevant timescale than that required for membrane disruption, and additionally may more accurately reflect intermediate levels of cell function. This type of assay could also provide information about peptide mechanisms by suggesting specifically impaired cellular functions, and indicate useful directions for further explorations of peptide mechanisms.

5.2 Permeabilization;

The terbium (III)/DPA interaction has previously been used to assess permeabilization in similar high-throughput vesicle screens[57]. One major advantage of this method is the fact that the chemistry is orthogonal to the translocation assay implemented here and therefore can be performed simultaneously on the same vesicle population. In order to implement this assay in the laboratory, current issues with terbium encapsulation and vesicle extrusion will need to be addressed. Vesicle production is inherently a temperamental procedure, so the previous difficulties in producing these vesicles may not indicate a fatal flaw. Ultimately, terbium is approximately 1% of the size of trypsin, so from a steric point of view it should not present any greater trouble with respect to encapsulation within vesicles or passage through membrane pores. It is possible that the charge on the ion contributes to the observed difficulties, although the salts of the buffer should minimize any such effects. In their high-throughput screen using Tb^{3+}/DPA interactions to report permeabilization, Marks et al used vesicles with a greater composition of PC relative to PG, which could also affect the ease of encapsulation[57]. It seems likely that successful implementation of this assay will simply require dedicated time and effort to determine conditions and adjustments for optimal vesicle production.

5.3 Translocation

Initial results adapting the vesicle based translocation assay to the high throughput plate format are promising, indicating a reasonable degree of internal consistency and ability to distinguish between translocating and non-translocating peptides. These data would be further supported by a systematic characterization of our DesHDAPs and their proline mutants using this

assay format. This complete series of experiments would allow a thorough comparison of the absolute values, consistency, and relative relationships between translocation abilities of peptides obtained using both the plate reader and fluorimeter assay systems. In the limited trials reported here, translocation values obtained from the plate reader do seem to be consistently higher than the equivalent values obtained from the fluorimeter, suggesting that direct comparison between instrumentation systems could be difficult. However, as long as relative values within a plate remain fairly consistent, this should not be overly problematic for the future of high-throughput screening because the most important comparisons will be those between peptides in the same library.

A bigger problem may arise from the delay between addition of peptide to solution and the onset of measurement. Two factors contribute to this delay: lag time inherent in the plate reader system and delays introduced by the sequential filling of wells. The former is likely to be more easily addressed than the latter. The delay between inserting the tray into the plate reader and pressing "read" and the onset of the first actual reading may be reducible by manipulating instrument and software settings appropriately. However, the inherent delay (and offset between wells) introduced by sequential addition of vesicles to wells is a more significant issue that will only increase in importance as the scale of this testing continues to increase. Generally, high-throughput formats can be used to interrogate time-sensitive kinetics assays if a multi-channel pipette is used to add solution to 8 or 12 wells simultaneously, thus dramatically reducing the time required to fill a plate. However, a significant volume of solution is required in order to be drawn up into a multi-channel pipette, effectively prohibiting the use of this instrument on volume-limited reagents. In this particular assay the vesicle solutions, particularly the control vesicles containing inhibited trypsin, are produced in a volume only just sufficient to fill the

wells. While vesicle production could be scaled up, both the DNS-PE lipid and the trypsin inhibitor are among the most expensive components of this assay and the multi-channel pipette troughs inevitably retain a non-trivial volume of wasted solution. Ultimately the ability to rapidly add solution to the wells of a plate may be one of the limiting factors in the scale of this assay. Extending the timecourse over which the change in fluorescence is monitored could minimize the importance of differences in start time. Monitoring for longer than 25 minutes was never considered feasible in fluorimeter-based experiments and therefore has not yet been explored on the plate reader. If the fluorescence were monitored and found to decrease consistently for longer periods such as one hour, differences of seconds or even minutes in initial peptide addition would presumably become virtually unimportant. In any case, when compared to the sequential nature of assays performed on the fluorimeter, the ability to perform even a dozen assays in parallel represents a significant and appreciable improvement in throughput.

5.4 Applications

Successful development of high-throughput screens for peptide activity and mechanism will be essential for the future of peptide screening and investigation in the both Elmore lab and more generally in the AMP field. Although these techniques can be used to enable screening of large peptide libraries, they can also be used to gather initial information about smaller sets of peptide variants in order to probe a particular question.

One area that has piqued the interest of AMP researchers is the effect of the identity of the charged residues found in polycationic AMPs. While both lysine and arginine carry a positive charge at physiological pH, the guanidinium group of arginine is capable of forming multiple hydrogen bonds, affecting its interactions with lipid membranes. Although predictions

would suggest that arginines would be highly unfavorable in transmembrane helices, both partitioning studies and mutagenic studies using proteins in biological systems confirm that arginine can and does function as part of transmembrane helices[85]. It is hypothesized that extensive hydrogen bonding to inwardly deformed lipid heads and water molecules may contribute to this phenomenon. Arginines are also common in permeabilizing AMPs and CPPs[86], supporting the fact that this residue can interact with lipid bilayers in meaningful ways.

In fact, there is evidence that not only the charge, but also the chemical properties of cationic side chains can affect the activity and mechanism of AMPs. Substitution studies with the AMP tritrpticin indicated that the identity of the cationic residues in a peptide could affect the peptide's mechanism of action[87]. By replacing arginines with lysines or unnatural amino acids with positively charged side chains, this study determined that residues capable of extensive hydrogen bonding interactions caused greater membrane disruption than equivalently charged residues unable to make those associations. Based on this information, it would be interesting to assess whether substituting arginine/lysine residues on BF2 or the designed peptides would affect their activity and/or mechanism of action. High-throughput screening would allow for rapid assessment of the many permutations and combinations of substitutions possible in these peptides.

The introduction of effective high-throughput screens will have the greatest impact on the ways in which novel AMPs are discovered. Previous work in the Elmore lab approached the design of new peptides by searching for fragments of histone sequences that conformed to given characteristics. Although all three peptides developed in this manner did display some antimicrobial activity, DesHDAP2 was a weak antimicrobial agent and was subsequently ignored for the mechanistic studies described earlier in this thesis. Furthermore, complete

characterization of these three peptides and their mechanisms required three years of study by multiple undergraduate researchers. High throughput screening techniques open the door for screening larger libraries of randomly or rationally designed peptides. Peptides identified by these screens with good activity and desirable mechanistic characteristics could then be carefully characterized using fluorimeter-based screens or used as the basis for new libraries. This type of approach could be used to explore the potential AMP activity of other histone fragments or to design a semi-random library of peptides with characteristics such as proline hinges or differing amphipathic character

Increased information from these studies may be able to expand the current understanding of what features contribute to effective antimicrobial peptides and determine particular mechanisms of action. This will ultimately enable more effective modification of existing peptides and design of novel peptides to address the need for novel antimicrobial agents for clinical applications.

1. Dougherty, T. & Pucci, M. J. *Handbook of Antibiotic Discovery and Development*. (Springer: 2012).
2. WHO | Antimicrobial resistance. *WHO* at <http://www.who.int/mediacentre/factsheets/fs194/en/>
3. Morell, E. A. & Balkin, D. M. Methicillin-Resistant Staphylococcus Aureus: A Pervasive Pathogen Highlights the Need for New Antimicrobial Development. *Yale J Biol Med* **83**, 223–233 (2010).
4. Otter, J. A. & French, G. L. Community-associated meticillin-resistant Staphylococcus aureus strains as a cause of healthcare-associated infection. *J. Hosp. Infect.* **79**, 189–193 (2011).
5. McManus, M. C. Mechanisms of bacterial resistance to antimicrobial agents. *Am J Health Syst Pharm* **54**, 1420–1433; quiz 1444–1446 (1997).
6. Proceedings of Local Branches of the Society of American Bacteriologists. *J Bacteriol* **51**, 125–129 (1946).
7. Ezekiel, D. H. & Hutchins, J. E. Mutations affecting RNA polymerase associated with rifampicin resistance in Escherichia coli. *Nature* **220**, 276–277 (1968).
8. Sigmund, C. D. & Morgan, E. A. Erythromycin resistance due to a mutation in a ribosomal RNA operon of Escherichia coli. *Proc. Natl. Acad. Sci. U.S.A.* **79**, 5602–5606 (1982).
9. Livermore, D. M. Discovery research: the scientific challenge of finding new antibiotics. *J. Antimicrob. Chemother.* **66**, 1941–1944 (2011).
10. Piddock, L. J. The crisis of no new antibiotics-what is the way forward? *Lancet Infect Dis* (2011).doi:10.1016/S1473-3099(11)70316-4
11. Park, I. Y., Park, C. B., Kim, M. S. & Kim, S. C. Parasin I, an antimicrobial peptide derived from histone H2A in the catfish, Parasilurus asotus. *FEBS Lett.* **437**, 258–262 (1998).
12. Birkemo, G. A., Lüders, T., Andersen, Ø., Nes, I. F. & Nissen-Meyer, J. Hipposin, a histone-derived antimicrobial peptide in Atlantic halibut (Hippoglossus hippoglossus L.). *Biochim. Biophys. Acta* **1646**, 207–215 (2003).
13. Park, C. B., Kim, M. S. & Kim, S. C. A novel antimicrobial peptide from Bufo bufo gargarizans. *Biochem. Biophys. Res. Commun.* **218**, 408–413 (1996).
14. Zasloff, M. Magainins, a class of antimicrobial peptides from Xenopus skin: isolation, characterization of two active forms, and partial cDNA sequence of a precursor. *Proc. Natl. Acad. Sci. U.S.A.* **84**, 5449–5453 (1987).
15. Slocinska, M., Marciniak, P. & Rosinski, G. Insects antiviral and anticancer peptides: new leads for the future? *Protein Pept. Lett.* **15**, 578–585 (2008).
16. Wiesner, J. & Vilcinskas, A. Antimicrobial peptides: the ancient arm of the human immune system. *Virulence* **1**, 440–464 (2010).
17. Wang, G., Li, X. & Wang, Z. APD2: the updated antimicrobial peptide database and its application in peptide design. *Nucleic Acids Research* **37**, D933–D937 (2009).
18. Janmey, P. A. & Kinnunen, P. K. J. Biophysical properties of lipids and dynamic membranes. *Trends Cell Biol.* **16**, 538–546 (2006).
19. Matsuzaki, K. Why and how are peptide-lipid interactions utilized for self-defense? Magainins and tachyplesins as archetypes. *Biochim. Biophys. Acta* **1462**, 1–10 (1999).
20. Jiang, Z. *et al.* Effects of net charge and the number of positively charged residues on the biological activity of amphipathic alpha-helical cationic antimicrobial peptides. *Biopolymers* **90**, 369–383 (2008).

21. Park, C. B., Kim, H. S. & Kim, S. C. Mechanism of action of the antimicrobial peptide buforin II: buforin II kills microorganisms by penetrating the cell membrane and inhibiting cellular functions. *Biochem. Biophys. Res. Commun.* **244**, 253–257 (1998).
22. Chen, Y. *et al.* Role of peptide hydrophobicity in the mechanism of action of alpha-helical antimicrobial peptides. *Antimicrob. Agents Chemother.* **51**, 1398–1406 (2007).
23. Tsao, H. S., Spinella, S. A., Lee, A. T. & Elmore, D. E. Design of novel histone-derived antimicrobial peptides. *Peptides* **30**, 2168–2173 (2009).
24. Hoskin, D. W. & Ramamoorthy, A. Studies on anticancer activities of antimicrobial peptides. *Biochim. Biophys. Acta* **1778**, 357–375 (2008).
25. Nizet, V. Antimicrobial peptide resistance mechanisms of human bacterial pathogens. *Curr Issues Mol Biol* **8**, 11–26 (2006).
26. Brogden, K. A. Antimicrobial peptides: pore formers or metabolic inhibitors in bacteria? *Nat. Rev. Microbiol.* **3**, 238–250 (2005).
27. Baumann, G. & Mueller, P. A molecular model of membrane excitability. *J. Supramol. Struct.* **2**, 538–557 (1974).
28. Matsuzaki, K., Murase, O., Fujii, N. & Miyajima, K. An antimicrobial peptide, magainin 2, induced rapid flip-flop of phospholipids coupled with pore formation and peptide translocation. *Biochemistry* **35**, 11361–11368 (1996).
29. Chen, Y. *et al.* Comparison of biophysical and biologic properties of alpha-helical enantiomeric antimicrobial peptides. *Chem Biol Drug Des* **67**, 162–173 (2006).
30. Subbalakshmi, C. & Sitaram, N. Mechanism of antimicrobial action of indolicidin. *FEMS Microbiol. Lett.* **160**, 91–96 (1998).
31. Park, K. H., Park, Y., Park, I.-S., Hahm, K.-S. & Shin, S. Y. Bacterial selectivity and plausible mode of antibacterial action of designed Pro-rich short model antimicrobial peptides. *J. Pept. Sci.* **14**, 876–882 (2008).
32. Park, C. B., Yi, K. S., Matsuzaki, K., Kim, M. S. & Kim, S. C. Structure-activity analysis of buforin II, a histone H2A-derived antimicrobial peptide: the proline hinge is responsible for the cell-penetrating ability of buforin II. *Proc. Natl. Acad. Sci. U.S.A.* **97**, 8245–8250 (2000).
33. Xie, Y., Fleming, E., Chen, J. L. & Elmore, D. E. Effect of proline position on the antimicrobial mechanism of buforin II. *Peptides* **32**, 677–682 (2011).
34. Uyterhoeven, E. T., Butler, C. H., Ko, D. & Elmore, D. E. Investigating the nucleic acid interactions and antimicrobial mechanism of buforin II. *FEBS Lett.* **582**, 1715–1718 (2008).
35. Lee, H. S. *et al.* Mechanism of anticancer activity of buforin IIb, a histone H2A-derived peptide. *Cancer Lett.* **271**, 47–55 (2008).
36. Kaouass, M., Beaulieu, R. & Balicki, D. Histonefection: Novel and potent non-viral gene delivery. *J Control Release* **113**, 245–254 (2006).
37. Kawasaki, H. & Iwamuro, S. Potential roles of histones in host defense as antimicrobial agents. *Infect Disord Drug Targets* **8**, 195–205 (2008).
38. Fernandes, J. M. O., Molle, G., Kemp, G. D. & Smith, V. J. Isolation and characterisation of oncorhyncin II, a histone H1-derived antimicrobial peptide from skin secretions of rainbow trout, Oncorhynchus mykiss. *Dev. Comp. Immunol.* **28**, 127–138 (2004).
39. Torchilin, V. P. Tat peptide-mediated intracellular delivery of pharmaceutical nanocarriers. *Adv. Drug Deliv. Rev.* **60**, 548–558 (2008).
40. Endoh, T. & Ohtsuki, T. Cellular siRNA delivery using cell-penetrating peptides modified for endosomal escape. *Adv. Drug Deliv. Rev.* **61**, 704–709 (2009).

41. Haas, A. K. *et al.* Human protein derived peptides for intracellular delivery of biomolecules. *The Biochemical Journal* (2011).doi:10.1042/BJ20111973
42. Tseng, Y.-L., Liu, J.-J. & Hong, R.-L. Translocation of liposomes into cancer cells by cell-penetrating peptides penetratin and tat: a kinetic and efficacy study. *Mol. Pharmacol.* **62**, 864–872 (2002).
43. Lindgren, M. & Langel, U. Classes and prediction of cell-penetrating peptides. *Methods Mol. Biol.* **683**, 3–19 (2011).
44. Fotin-Mleczek, M., Fischer, R. & Brock, R. Endocytosis and cationic cell-penetrating peptides--a merger of concepts and methods. *Curr. Pharm. Des.* **11**, 3613–3628 (2005).
45. Lundin, P. *et al.* Distinct Uptake Routes of Cell-Penetrating Peptide Conjugates. *Bioconjugate Chem.* **19**, 2535–2542 (2008).
46. Martín, I., Teixidó, M. & Giralt, E. Design, Synthesis and Characterization of a New Anionic Cell-Penetrating Peptide: SAP(E). *ChemBioChem* **12**, 896–903 (2011).
47. Bland, J. M., De Lucca, A. J., Jacks, T. J. & Vigo, C. B. All-D-cecropin B: synthesis, conformation, lipopolysaccharide binding, and antibacterial activity. *Mol. Cell. Biochem.* **218**, 105–111 (2001).
48. Hamamoto, K., Kida, Y., Zhang, Y., Shimizu, T. & Kuwano, K. Antimicrobial activity and stability to proteolysis of small linear cationic peptides with D-amino acid substitutions. *Microbiol. Immunol.* **46**, 741–749 (2002).
49. De Lucca, A. J. *et al.* D-cecropin B: proteolytic resistance, lethality for pathogenic fungi and binding properties. *Med. Mycol.* **38**, 301–308 (2000).
50. Chen, Y., Mant, C. T. & Hodges, R. S. Determination of stereochemistry stability coefficients of amino acid side-chains in an amphipathic α-helix. *The Journal of Peptide Research* **59**, 18–33 (2002).
51. Meng, H. & Kumar, K. Antimicrobial activity and protease stability of peptides containing fluorinated amino acids. *J. Am. Chem. Soc.* **129**, 15615–15622 (2007).
52. Xie, Q. *et al.* In vitro system for high-throughput screening of random peptide libraries for antimicrobial peptides that recognize bacterial membranes. *J. Pept. Sci.* **12**, 643–652 (2006).
53. Kim, Y. S. & Cha, H. J. High-throughput and facile assay of antimicrobial peptides using pH-controlled fluorescence resonance energy transfer. *Antimicrob. Agents Chemother.* **50**, 3330–3335 (2006).
54. Brodin, P. & Christophe, T. High-content screening in infectious diseases. *Curr Opin Chem Biol* **15**, 534–539 (2011).
55. Rathinakumar, R. & Wimley, W. C. Biomolecular engineering by combinatorial design and high-throughput screening: small, soluble peptides that permeabilize membranes. *J. Am. Chem. Soc.* **130**, 9849–9858 (2008).
56. Rathinakumar, R., Walkenhorst, W. F. & Wimley, W. C. Broad-spectrum antimicrobial peptides by rational combinatorial design and high-throughput screening: the importance of interfacial activity. *J. Am. Chem. Soc.* **131**, 7609–7617 (2009).
57. Marks, J. R., Placone, J., Hristova, K. & Wimley, W. C. Spontaneous membrane-translocating peptides by orthogonal high-throughput screening. *J. Am. Chem. Soc.* **133**, 8995–9004 (2011).
58. Kobayashi, S., Takeshima, K., Park, C. B., Kim, S. C. & Matsuzaki, K. Interactions of the novel antimicrobial peptide buforin 2 with lipid bilayers: proline as a translocation promoting factor. *Biochemistry* **39**, 8648–8654 (2000).

59. Kobayashi, S. *et al.* Membrane translocation mechanism of the antimicrobial peptide buforin 2. *Biochemistry* **43**, 15610–15616 (2004).
60. Katsumi, M. Magainins as paradigm for the mode of action of pore forming polypeptides. *Biochimica et Biophysica Acta (BBA) - Reviews on Biomembranes* **1376**, 391–400 (1998).
61. Lee, S.-A. *et al.* Solution structure and cell selectivity of piscidin 1 and its analogues. *Biochemistry* **46**, 3653–3663 (2007).
62. Thennarasu, S. & Nagaraj, R. Specific antimicrobial and hemolytic activities of 18-residue peptides derived from the amino terminal region of the toxin pardaxin. *Protein Eng.* **9**, 1219–1224 (1996).
63. Zhang, L., Benz, R. & Hancock, R. E. Influence of proline residues on the antibacterial and synergistic activities of alpha-helical peptides. *Biochemistry* **38**, 8102–8111 (1999).
64. GOUREVITCH, A., TYNDA, J. M., PUGLISI, T. A. & LEIN, J. Studies on the mechanism of action of kanamycin. *Antibiot Annu* **6**, 784–789 (1958).
65. Misumi, M. & Tanaka, N. Mechanism of inhibition of translocation by kanamycin and viomycin: a comparative study with fusidic acid. *Biochem. Biophys. Res. Commun.* **92**, 647–654 (1980).
66. Pestka, S. The use of inhibitors in studies on protein synthesis. *Meth. Enzymol.* **30**, 261–282 (1974).
67. O'Brien, M. C. & Bolton, W. E. Comparison of cell viability probes compatible with fixation and permeabilization for combined surface and intracellular staining in flow cytometry. *Cytometry* **19**, 243–255 (1995).
68. Szabó, G., Jr, Kiss, A. & Trón, L. Permeabilization of lymphocytes with polyethylene glycol 1000. Discrimination of permeabilized cells by flow cytometry. *Cytometry* **3**, 59–63 (1982).
69. Darzynkiewicz, Z. *et al.* Features of apoptotic cells measured by flow cytometry. *Cytometry* **13**, 795–808 (1992).
70. Molecular Probes LIVE/DEAD BacLight Bacterial Cell Viability Tests. (2004).at <http://www.invitrogen.com/site/us/en/home/References/Molecular-Probes-The-Handbook/Assays-for-Cell-Viability-Proliferation-and-Function/Viability-and-Cytotoxicity-Assay-Kits-for-Diverse-Cell-Types.html>
71. Rodnina, M. V., Beringer, M. & Wintermeyer, W. How ribosomes make peptide bonds. *Trends Biochem. Sci.* **32**, 20–26 (2007).
72. Song, K.-M. *et al.* Gold nanoparticle-based colorimetric detection of kanamycin using a DNA aptamer. *Anal. Biochem.* **415**, 175–181 (2011).
73. Rathinakumar, R. & Wimley, W. C. High-throughput discovery of broad-spectrum peptide antibiotics. *FASEB J.* **24**, 3232–3238 (2010).
74. Campbell, J. High-throughput assessment of bacterial growth inhibition by optical density measurements. *Curr Protoc Chem Biol* **3**, (2011).
75. Lan, Y. *et al.* Structural contributions to the intracellular targeting strategies of antimicrobial peptides. *Biochim. Biophys. Acta* **1798**, 1934–1943 (2010).
76. Hamann, S. *et al.* Measurement of Cell Volume Changes by Fluorescence Self-Quenching. *Journal of Fluorescence* **12**, 139–145 (2002).
77. Chen, R. F. & Knutson, J. R. Mechanism of fluorescence concentration quenching of carboxyfluorescein in liposomes: Energy transfer to nonfluorescent dimers. *Analytical Biochemistry* **172**, 61–77 (1988).
78. Torchilin, V. P. & Weissig, V. *Liposomes: a practical approach*. (Oxford University Press: 2003).

79. Wallach, D. F. H., Surgenor, D. M., Soderberg, J. & Delano, E. Preparation and Properties of 3,6-Dihydroxy-2,4-bis-[N-N'-di-(carboxymethyl)-aminomethyl] fluoran. *Anal. Chem.* **31**, 456–460 (1959).
80. Memoli, A., Palermiti, L. G., Travagli, V. & Alhaique, F. Effects of surfactants on the spectral behaviour of calcein (II): a method of evaluation. *Journal of Pharmaceutical and Biomedical Analysis* **19**, 627–632 (1999).
81. Wilschut, J., Düzgüneş, N., Fraley, R. & Papahadjopoulos, D. Studies on the mechanism of membrane fusion: kinetics of calcium ion induced fusion of phosphatidylserine vesicles followed by a new assay for mixing of aqueous vesicle contents. *Biochemistry* **19**, 6011–6021 (1980).
82. Spinella, S. A., Nelson, R. B. & Elmore, D. E. Measuring Peptide Translocation into Large Unilamellar Vesicles. *Journal of Visualized Experiments* (2012).doi:10.3791/3571
83. Mosmann, T. Rapid colorimetric assay for cellular growth and survival: application to proliferation and cytotoxicity assays. *J. Immunol. Methods* **65**, 55–63 (1983).
84. Coder, D. M. Assessment of Cell Viability. *Current Protocols in Cytometry* at <http://onlinelibrary.wiley.com/doi/10.1002/0471142956.cy0902s15/abstract>
85. Hristova, K. & Wimley, W. C. A look at arginine in membranes. *J. Membr. Biol.* **239**, 49–56 (2011).
86. Han, X. & Kang, W. Sequence analysis and membrane partitioning energies of alpha-helical antimicrobial peptides. *Bioinformatics* **20**, 970–973 (2004).
87. Nguyen, L. T., de Boer, L., Zaat, S. A. J. & Vogel, H. J. Investigating the cationic side chains of the antimicrobial peptide tritrpticin: Hydrogen bonding properties govern its membrane-disruptive activities. *Biochimica et Biophysica Acta (BBA) - Biomembranes* **1808**, 2297–2303 (2011).